IDA PAPER P-2533

IDA GAMMA-RAY LASER ANNUAL SUMMARY REPORT (1990)

Investigation of the Feasibility of Developing a Laser Using Nuclear Transitions

Bohdan Balko
Irvin W. Kay

April 1992

Prepared for
Strategic Defense Initiative Organization
Innovative Science and Technology Office

Dwight Duston, *Director*

INSTITUTE FOR DEFENSE ANALYSES
1801 N. Beauregard Street, Alexandria, Virginia 22311-1772

IDA Log No. HQ 90-36742

DEFINITIONS

IDA publishes the following documents to report the results of its work.

Reports

Reports are the most authoritative and most carefully considered products IDA publishes. They normally embody results of major projects which (a) have a direct bearing on decisions affecting major programs, (b) address issues of significant concern to the Executive Branch, the Congress and/or the public, or (c) address issues that have significant economic implications. IDA Reports are reviewed by outside panels of experts to ensure their high quality and relevance to the problems studied, and they are released by the President of IDA.

Group Reports

Group Reports record the findings and results of IDA established working groups and panels composed of senior individuals addressing major issues which otherwise would be the subject of an IDA Report. IDA Group Reports are reviewed by the senior individuals responsible for the project and others as selected by IDA to ensure their high quality and relevance to the problems studied, and are released by the President of IDA.

Papers

Papers, also authoritative and carefully considered products of IDA, address studies that are narrower in scope than those covered in Reports. IDA Papers are reviewed to ensure that they meet the high standards expected of refereed papers in professional journals or formal Agency reports.

Documents

IDA Documents are used for the convenience of the sponsors or the analysts (a) to record substantive work done in quick reaction studies, (b) to record the proceedings of conferences and meetings, (c) to make available preliminary and tentative results of analyses, (d) to record data developed in the course of an investigation, or (e) to forward information that is essentially unanalyzed and unevaluated. The review of IDA Documents is suited to their content and intended use.

The work reported in this document was conducted under contract MDA 903 89 C 0003 for the Department of Defense. The publication of this IDA Paper does not indicate endorsement by the Department of Defense, nor should the contents be construed as reflecting the official position of that Agency.

REPORT DOCUMENTATION PAGE

Form Approved
OMB No. 0704-0188

1. AGENCY USE ONLY *(Leave blank)*	2. REPORT DATE	3. REPORT TYPE AND DATES COVERED
	April 1992	Final--January 1991-March 1992

4. TITLE AND SUBTITLE
IDA Gamma-Ray Laser Annual Summary Report (1990): Investigation of the Feasibility of Developing a Laser Using Nuclear Transitions

5. FUNDING NUMBERS
C - MDA 903 89 C 0003

T- T-R2-597.03

6. AUTHOR(S)
Bohdan Balko, Irvin W. Kay

7. PERFORMING ORGANIZATION NAME(S) AND ADDRESS(ES)
Institute for Defense Analyses
1801 N. Beauregard St.
Alexandria, VA 22311-1772

8. PERFORMING ORGANIZATION REPORT NUMBER
IDA Paper P-2533

9. SPONSORING/MONITORING AGENCY NAME(S) AND ADDRESS(ES)
Strategic Defense Initiative Organization
Innovative Science and Technology Office
The Pentagon, Room 1E167
Washington, DC 20301-7100

10. SPONSORING/MONITORING AGENCY REPORT NUMBER

11. SUPPLEMENTARY NOTES

12a. DISTRIBUTION/AVAILABILITY STATEMENT
Approved for public release; distribution unlimited.

12b. DISTRIBUTION CODE

13. ABSTRACT *(Maximum 200 words)*

This paper compares two processes that can occur, under different conditions, in the same system of nuclei: amplified spontaneous emission (ASE) and superfluorescence (SF). It concludes that the (Trammell and Hannon) conditions for the occurrence of ASE are more restrictive than those for the occurrence of SF. Therefore, the conclusion by some authors based on an analysis of ASE, that coherent electromagnetic emission from a nuclear system is not feasible, is incorrect. The paper examines the feasibility of nuclear SF in ^{60}Co. It concludes that SF will occur in the excited state obtained by thermal neutron pumping with fluxes ranging from 10^{18} to 10^{23} neutrons per second.

14. SUBJECT TERMS
gamma-ray laser, graser, nuclear superfluorescence (SF), amplified spontaneous emission (ASE), nuclear isomers, proposed nuclear SF experiment, parametric fits to Monte Carlo SF results

15. NUMBER OF PAGES
64

16. PRICE CODE

17. SECURITY CLASSIFICATION OF REPORT	18. SECURITY CLASSIFICATION OF THIS PAGE	19. SECURITY CLASSIFICATION OF ABSTRACT	20. LIMITATION OF ABSTRACT
UNCLASSIFIED	UNCLASSIFIED	UNCLASSIFIED	SAR

IDA PAPER P-2533

IDA GAMMA-RAY LASER ANNUAL SUMMARY REPORT (1990)

Investigation of the Feasibility of Developing a Laser Using Nuclear Transitions

Bohdan Balko
Irvin W. Kay

April 1992

INSTITUTE FOR DEFENSE ANALYSES
Contract MDA 903 89 C 0003
Task T-R2-597.03

PREFACE

In January 1985 the Director of the Science and Technology Directorate of the Strategic Defense Initiative Organization (SDIO) asked members of the IDA research staff to investigate the feasibility of developing a γ-ray laser. The staff determined what work had been done, who was currently working in the field, and what work should be encouraged or supported. A workshop was convened for researchers directly involved both in gamma-ray laser work and in ancillary fields such as nuclear structure, radiation propagation in crystals, Mössbauer Effect, and optical lasers. Next, an in-house study was undertaken to clarify critical issues concerning the various pumping schemes proposed at the workshop as well as systems questions about the γ-ray laser as a working device.

The proceedings of the workshop were published in the form of a report to the Innovative Science and Technology Office (IST) of the SDIO. The work completed in 1985 was presented in IDA Paper P-2021.

In 1986, the in-house work focused on extending the data base, the nature of superradiance in the γ-ray laser context, and a detailed investigation of the upconversion pumping scheme. A discussion of nuclear systematics, investigations of electron-nuclear-driven pumping, and lifetime measurements rounded out that study. The results of the FY1986 effort were presented in IDA Paper P-2004.

In 1987, the IDA research staff looked at the state of the art and assessed the situation in γ-ray laser work with focus on two areas of research interest critical to concepts for developing a γ-ray laser. Heating effects associated with upconversion techniques were discussed. The sources of inhomogeneous broadening which destroy the Mössbauer Effect were investigated and techniques available for restoring the resonance by external or internal fields were considered (IDA Paper P-2083).

In 1988, the in-house work concentrated on (1) establishing a theoretical model of nuclear superfluorescence that took into account specific characteristics of nuclear radiation emission and transport that are important for superfluorescence on the nuclear scale, (2) examining in more detail and for more realistic parameters the heating effects inherent in

upconversion concepts, and (3) examining the speed of response of nuclei to applied external fields, as exhibited by their spectra (IDA Paper P-2175).

In 1989 the work concentrated on developing a model of nuclear superfluorescence that included:

1. Multilevel systems,
2. Incoherent pumping at finite rates,
3. Spatial attenuation of the electromagnetic field in the active region,
4. Dephasing due to inhomogeneous broadening,
5. Population depletion due to competing processes like internal conversion and spontaneous transverse emission.

This was done by generalizing the Haake-Reibold model of superfluorescence based on Maxwell-Bloch equations. The effects of inhomogeneous broadening on superfluorescence were studied using a theory developed by J. Eberly. The enhancement of superfluorescence in inhomogeneously broadened systems by time-dependent hyperfine interactions was investigated using the theory developed by M. Blume. We also investigated coherent aspects of nuclear emission and absorption in the presence of homogeneous and inhomogeneous broadening of source and absorber (IDA Paper P-2335).

The present document describes the 1990 work in which we applied the Maxwell-Bloch model (and other models) of the interaction of the electromagnetic field with matter to the γ-ray laser problem in the following way:

1. We compared amplified spontaneous emission (ASE) and superfluorescence (SF) within the same model and found the conditions for SF to be more easily attainable.
2. We analyzed the feasibility of SF in a real nucleus, ^{60}Co assumed prepared in the isomeric (inverted) state through a thermal neutron reaction with the parent, and calculated SF pulse intensity under different conditions. This is the first published result of a real nucleus, pumped through an existing mechanism and achievable fluxes of the pumping radiation, to give a SF pulse.
3. From the Monte Carlo runs with the Maxwell-Bloch equations we developed parametric equations characterizing the SF emission delay time. The parametric equations simplify future analyses of SF phenomena.
4. We tested the popular assumption that SF in an attenuating medium can be modeled by assuming a reduction in the effective length of the cylindrical active

volume, in effect assuming the number of collective radiators to be proportional to the inverse of the attenuation coefficient. This assumption proved to be inaccurate and unacceptable for candidate selection.

The development of a γ-ray laser is viewed as a high-risk/high-payoff undertaking. IDA's involvement focuses on minimizing the risk and on striving to redirect the effort when proposed schemes are shown not to be feasible.

ABSTRACT

This paper compares two processes that can occur, under different conditions, in the same system of nuclei: amplified spontaneous emission (ASE) and superfluorescence (SF). It concludes that the (Trammell and Hannon) conditions for the occurrence of ASE are more restrictive than those for the occurrence of SF. Therefore, the conclusion by some authors based on an analysis of ASE, that coherent electromagnetic emission from a nuclear system is not feasible, is incorrect. The paper examines the feasibility of nuclear SF in ^{60}Co. It concludes that SF will occur in the excited state obtained by thermal neutron pumping with fluxes ranging from 10^{18} to 10^{23} neutrons per second.

CONTENTS

FIGURES

TABLES

SUMMARY

This report describes the 1990 research effort by members of the IDA staff in the field of γ-ray lasers. The work is part of a continuing task in support of the Innovative Science and Technology Office (IST) of the Strategic Defense Initiative Organization (SDIO). The development of a γ-ray laser is a high-risk science and technology undertaking. IDA involvement has focused in large measure on minimizing the risk and attempting to redirect the program as quickly as possible when proposed schemes prove infeasible.

In this report we look for optimal and realistic conditions for the emission of coherent electromagnetic radiation from nuclei and the development of a γ-ray laser. We compare the requirements for amplified spontaneous emission (ASE), or pulsed laser emission, with superfluorescence (SF), a cooperative emission from an inverted population of nuclei. We find the requirements for SF less restrictive on the nuclear and solid state properties of the active medium. Finally we use the general theory of SF to examine the feasibility of nuclear SF in ^{60}Co obtained in the excited state by thermal neutron pumping with fluxes ranging from 10^{17} to 10^{23} neutrons/sec. It should be emphasized that our calculation is based on real properties of materials and that this is the first calculation published, to our knowledge, that includes broadening effects, attenuation, coupling transitions and finite pumping times in a single model.

The interaction of the radiation field with matter leads to coherent emission (ASE) and cooperative emission (SF) in the same inverted amplification medium. The two phenomena can be distinguished theoretically and experimentally. The selection of appropriate candidate nuclei depends on the specific phenomena because of the different requirements that have to be met. We found that the SF process for nuclei is less restrictive, whereas researchers have generally used the Schawlow-Townes threshold condition for ASE as a guideline for selecting candidates. The Schawlow-Townes condition is derived in the linear approximation whereas we use the full nonlinear interaction Hamiltonian to obtain our results.

We concentrated on the SF process and studied the requirements for SF pulse emission as a function of the number of cooperating nuclei, the attenuation properties of the

medium, the natural single nuclear lifetime and the pumping rate. We characterize the emitted pulses by the delay time and the intensity and use the results from the Monte Carlo solutions of the Maxwell-Bloch equations to obtain parametric equations for the delay time. This allows us to make predictions and perform certain analyses much more easily without additional time-consuming Monte Carlo calculations.

A popular approach for taking into account the attenuation of the medium has been to assume a reduction in the active volume by the inverse of the attenuation coefficient. We checked this assumption by performing the complete Monte Carlo calculation of the Maxwell-Bloch equations and found a discrepancy of a factor of four in the delay time calculations. The Monte Carlo calculation gave shorter delay times than the volume reduction model. This difference could lead to a critical error in the candidate selection process and rule out certain nuclei that could in fact be useful.

I. INTRODUCTION

In the history of γ-ray laser research, initially, attention focused on the search for concepts and nuclei that satisfied the Schawlow-Townes (S-T) condition for lasing, which can occur either in the form of continuous wave (CW) or pulsed emission. Lasing in the form of pulse emission initiated by spontaneous decay processes is usually referred to as amplified spontaneous emission (ASE). Recognition that in the nuclear regime ASE is a more realistic phenomenon to expect than CW lasing changed the direction of the γ-ray laser research.

Trammell and Hannon (Ref. 1) analyzed the conditions required for the occurrence of ASE and found that it is a more restricted process than lasing and is limited by a modified version of cooperative emission following inversion, the S-T condition. They also drew a similar conclusion about the phenomenon of superfluorescence (SF); however, reasons for disagreeing with that inference are discussed in Chapter III.

More recently SF was considered a more feasible and promising approach to nuclear lasing (Ref. 2). In subsequent investigations the processes of ASE and SF have been treated in more detail and generality. The transition region between ASE and SF has also been investigated experimentally in atomic systems (Ref. 3a, b). Such studies provide the background and permit comparisons of ASE and SF in nuclear systems leading to valid checks on candidates for experimentally demonstrable feasibility of ASE or SF.

Nevertheless, not all of the important physical effects that should be taken into account in the analysis of real nuclear systems have been considered in a single theory. The most complete theory for treating nuclear SF was presented in IDA paper P-2335 and is used in our analysis.

In Chapter II we compare the necessary conditions for the existence of the phenomena ASE as modeled by Trammell and Hannon and SF and show that the occurrence of SF is more probable for the nuclear case under certain conditions.

Chapter III deals with the details of a parametric description of the SF processes, (derived from the Monte Carlo calculations given in Ref. 4). This approach permits investigations of SF phenomena without resort to the lengthy calculations of Ref. 4.

Chapter IV uses the earlier theoretical development to investigate the feasibility of SF in a real nucleus, ^{60}Co.

II. COMPARISON OF AMPLIFIED SPONTANEOUS EMISSION AS MODELED BY TRAMMELL AND HANNON AND SUPERFLUORESCENCE

A. LASING (AMPLIFIED SPONTANEOUS EMISSION)

ASE can be viewed as a transport process with gain. It is governed, as is lasing in general, by the Schawlow-Townes threshold condition (Ref. 1) which simply states that for gain to occur in a region, the stimulation of photons has to exceed the absorption. For this to occur, the gain coefficient has to be positive:

$$K = \sigma_s \Delta n^* - \mu > 0 \quad ,$$

where the stimulation cross-section σ_s is given by

$$\sigma_s = \frac{\lambda^2}{2\pi} \frac{f g_N \beta}{(1+a)(1+\alpha)} \quad , \tag{1}$$

and

Δn^* = inversion,

μ = linear attenuation coefficient,

β = branching ratio,

λ = the wavelength of the emission,

a = inhomogeneous broadening parameter,

α = internal conversion coefficient,

f = recoilless fraction.

The Schawlow-Townes condition sets the threshold for the occurrence of both lasing and ASE. The basic process is a transport process independent of time (this is strictly true only for a steady state operation). For a pulsed laser or ASE the conditions must allow for the fact that the population of the excited level decreases during emission. Only the inversion Δn^* changes; the other parameters in the Schawlow-Townes condition

are independent of time. This is discussed by Trammell and Hannon in Ref. 1, where the threshold condition for pulsed lasers is derived. We use their results in our comparison of ASE and superfluorescence (SF). We also extend their calculations into regions of particular interest and present the results in Appendix A.

B. SUPERFLUORESCENCE

SF can be viewed as a spontaneous emission by coupled, cooperating radiators. The process is initiated by quantum fluctuations of the vacuum electromagnetic field, or the emission of a photon, which gives rise to a phasing or build up of correlations in the inverted region. SF is governed by the dynamics of the evolving system as described, for example, by the Maxwell-Bloch equations with random noise sources (Ref. 4, Chapter I). No simple threshold condition connecting the pertinent parameters exists as in the case of lasing. Conditions for the occurrence of SF are described in terms of characteristic times representing the speed of competing processes: namely, the single nucleus lifetime τ_n, the radiative lifetime τ_r, the cooperation time τ_c, the time of emission of the SF pulse τ_{SF}, the delay time of the pulse τ_D, and the dephasing time[1] τ_ϕ and the pumping time τ_γ. The cooperation time[2] τ_c sets the absolute upper limit on the SF time τ_{SF} and consequently on the delay time τ_D. We discuss this in the next section. Intuitively one expects that for SF to occur the following conditions should hold:

$$\tau_\gamma < \tau_D < \tau_\phi, \tau_n, \tau_c \quad .$$

More rigorous analysis (Ref. 5) shows that

$$\sqrt{\tau_D \tau_{SF}} < \tau_\phi$$

is actually the appropriate condition between the delay time, SF time, and the dephasing time.

---

1 This commonly is due to collisions or inhomogenous broadening.

2 The cooperation time is obtained from the Dicke formula for the emission rate, $\gamma_c = \frac{1}{4} N_c \frac{1}{\tau_r} \lambda 2 / A$, where N_c is the number of emitters, λ the linewidth of the radiation and A the cross section of the rod forming the inverted region and a self consistent argument determining how many atoms can be covered by the emission of a single atom during the Dicke emission time, $\frac{1}{\gamma_c}$. With $N_c = \left(\frac{c}{\gamma_c}\right) A\rho$ we get $\tau_c = \sqrt{\frac{2}{c\rho\Gamma\lambda^2}}$.

These times are defined in terms of elementary parameters or derived from basic theories (Refs. 5, 6, 7). For our purposes they are as follows:

$$\tau_r = \alpha\tau_n \quad ,$$

$$\tau_c = \frac{2}{\sqrt{c\rho\Gamma\lambda^2}} \quad ,$$

$$\tau_{SF} = \frac{8\pi}{3}\frac{1}{\lambda^2\rho l}\tau_r \quad , \tag{2}$$

$$\tau_D = \frac{1}{2}\tau_{SF}\, ln(N) \quad ,$$

$$\tau_\phi = \frac{\tau_n}{a} \quad ,$$

$$\tau_\gamma = \frac{1}{\gamma} \quad ,$$

where γ is the single nucleus spontaneous pumping rate producing the inversion, Γ is the single nucleus spontaneous radiative rate, ρ is the nuclear density, a is the inhomogeneous broadening parameter (Ref. 1) defined by $\Gamma_\beta = (1+a)\,\Gamma_n$, and l the length of the active region. The expressions of τ_{SF} and τ_D given in Eqs. (6) and (7) are model dependent and are used here for convenience (see, for example, Ref. 8 or Chapter III). The phenomena of SF is discussed in greater detail in Refs. 9 and 10.

Using the Maxwell-Bloch equations with stochastic sources (Ref. 4, Chapter I), we have studied the feasibility of nuclear SF. This formalism characterizes SF under physically meaningful conditions. Processes important to nuclear SF such as attenuation, inhomogeneous line broadening and competing transitions are all easily and naturally incorporated. The formalism also allows consideration of finite pumping times and incoherent pumping mechanisms. Using the delay time, τ_D, as the criterion for the strength of SF emission, we found the effective length l_{eff} of the active medium for dissipative systems ($\mu \neq 0$) to be about $l_{eff} = \frac{4}{\mu}$ (or higher) instead of $\frac{1}{\mu}$ as is often assumed (Refs. 1, 11). We used the Maxwell-Bloch equations and the Eberly theory (Ref. 7) to study the effect of inhomogeneous broadening, another phenomenon critical in the generation of nuclear SF. Inhomogeneous broadening produces dephasing with a characteristic time of τ_ϕ, so that at short times after inversion ($\tau << \tau_\phi$) the effect on SF of inhomogeneous broadening is small (increasing with time), but not constant. In the equation for σ_s and the

gain coefficient (the Schawlow-Townes condition), the effect of inhomogeneous broadening is a constant reduction factor $\left(\frac{1}{1+a}\right)$. Thus SF and lasing are quite different in this respect: both the attenuation and inhomogeneous broadening play a different, and as will be seen, less restrictive role in the SF process than in the lasing process.

C. LIMIT ON THE COOPERATION LENGTH

The absolute upper limit on effective length of the active medium can be found from the cooperation time. The cooperation time is determined by the number of nuclei that can interact within the lifetime of the nuclear state (Ref. 6). From Eq. (2) we have

$$\tau_c = \frac{2}{\sqrt{c\rho\Gamma\lambda^2}} = 2\sqrt{\frac{\tau_r}{c\rho\lambda^2}} \quad . \tag{3}$$

where $\Gamma = \frac{1}{\tau_r}$ is the radiative rate.

The maximum effective length has to be less than the correlation length, i.e.,

$$l < l_c = \tau_c c = 2\sqrt{\frac{c\tau_r}{\rho\lambda^2}} \quad . \tag{4}$$

From this we can get the absolute limit on the SF time:

$$\tau_{SF} \geq \left(\frac{8\pi}{3}\right)\frac{1}{\lambda^2 \rho l_c}\tau_r = \left(\frac{8\pi}{3}\right)\left(\frac{1}{\lambda^2\rho}\right)\frac{1}{2}\sqrt{\frac{\rho\lambda^2}{c\tau_r}}\,\tau_r = \left(\frac{4\pi}{3}\right)\sqrt{\frac{\alpha\tau_n}{c\rho\lambda^2}} \quad . \tag{5}$$

Using typical nuclear parameters,

$$\rho = 10^{22} \ ,$$

$$\lambda = 1A = 10^{-8}\text{cm} \ ,$$

$$\alpha = 10 \ ,$$

$$c = 3 \times 10^{10}\text{cm/sec} \ ,$$

$$c\rho\lambda^2 = 3 \times 10^{16}\ \text{sec}^{-1} \ ,$$

and assuming f = 1, we get

$$\tau_{SF} \geq \left(\frac{4\pi}{3}\right) \frac{10^{-8}}{1.8} \sqrt{\tau_n} = 2.3 \times 10^{-8} \sqrt{\tau_n} \quad . \tag{6}$$

This gives the minimum SF pulse emission time. Generally the experimentally observed pulse emission time is greater than τ_{SF}.

D. COMPARISON OF CONDITIONS ON ASE AND SF

For the steady state laser the Schawlow-Townes gain condition is

$$K = \frac{\lambda^2}{2\pi} \frac{f \Delta n^*}{(1+\alpha)(1+a)} - \mu > 0 \quad . \tag{7}$$

As shown by Trammell and Hannon (Ref. 1), this has to be modified for the pulsed laser, or ASE, to account for the reductions in the inversion during emission.[3] Their results show that a factor of 21 multiplying μ in the condition on K is required,[4] thus for the present discussion we assume that

$$K = \frac{\lambda^2}{2\pi} \frac{f \Delta n^*}{(1+\alpha)(1+a)} - 21\mu > 0 \tag{8}$$

for a pulsed laser.

Assuming $\alpha >> 1$, $a >> 1$,

we get

$$\frac{\lambda^2}{2\pi} \frac{f \Delta n^*}{a\alpha (21) \mu} > 1$$

and finally

$$\alpha a \mu < \frac{\lambda^2 f \Delta n^*}{2\pi(21)} \quad .$$

---

3 This is the same as the well-known "laser lethargy" of M. Scully and F. Hoffman.

4 This condition has limited applicability to systems where the decrease in inversion is assumed to be due to the natural decay process. For high-gain systems the factor of 21 increases, as we discovered in our investigations when we generalized the results of Trammell and Hannon (see Appendix A).

The SF condition requires that SF dynamics are faster than dephasing or depopulating processes. We assume $\tau_\gamma \approx 0$ and use

$$\sqrt{\tau_D \tau_{SF}} < \tau_\phi \text{ and } \tau_D < \tau_c \tag{9}$$

as the mathematical statement of this condition.

Assuming an effective length $l_{eff} = \frac{4}{\mu}$, for $\mu \neq 0$, as determined by calculations based on the Maxwell-Bloch equations (Ref. 4)[5] using $\tau_\phi = \frac{\tau_n}{a}$, $\tau_r = \alpha\tau_n$ and applying the above criteria we get:

$$\left(\frac{1}{2}\tau_{SF}\, ln\,(N)\,\tau_{SF}\right)^{\frac{1}{2}} < \frac{\tau_n}{a} ,$$

or

$$\sqrt{\frac{1}{2}}\,\tau_{SF}\sqrt{ln\,(N)} < \frac{\tau_n}{a} .$$

$$\sqrt{\frac{1}{2}}\left(\frac{8\pi}{3}\right)\frac{1}{\lambda^2 f\rho l}\,\tau_r\,\sqrt{ln\,N} < \frac{\tau_n}{a} ,$$

or

$$\frac{4\sqrt{2}}{3}\,\frac{\pi\mu\alpha\tau_n}{\lambda^2 f\rho\,(4)}\,\sqrt{ln\,N} < \frac{\tau_n}{a} ,$$

i.e.,

$$4\,\frac{\sqrt{2}}{12}\,\frac{\pi\mu\alpha a}{\lambda^2 f\rho}\sqrt{ln\,(N)} < 1 ,$$

and therefore

$$(\mu\,\alpha\,a) < \frac{3\lambda^2 f\rho}{\pi\sqrt{2\,ln\,(N)}} . \tag{10}$$

---

5 Detailed calculations are given in Chapter III.

In making the comparison between SF and ASE we will consider the constraints on the product (α a μ) for the competing processes. The internal conversion coefficient α is a given for a particular nuclear isomer, and we don't have a lot of external control over the existing value.[6] Nevertheless, it is an important parameter for candidate selection. The inhomogeneous broadening represented by a, on the other hand, can be controlled by external RF pulses and other techniques, and the linear attenuation coefficient μ can be reduced through the Borrmann Effect. Conveniently, the product (α a μ) appears in the requirements for both ASE and SF processes.

The constraint on ASE is

$$\alpha\, a\, \mu < \frac{\lambda^2 f \Delta n^*}{2\pi\,(21)} \quad , \tag{11}$$

and on the SF process

$$\alpha\, a\, \mu < \frac{3\lambda^2 f \rho}{\pi\sqrt{2l n\,(N)}} \quad . \tag{12}$$

Taking the ratio of the right-hand sides of Eqs. (11) and (12) we get

$$R = \frac{3\lambda^2 \rho}{\pi\sqrt{2l n(N)}} \Big/ \frac{\lambda^2 \Delta n^*}{2\pi(21)} \quad , \tag{13}$$

which reduces to

$$R = \frac{126}{\sqrt{2l n(N)}} = \frac{89.095}{\sqrt{l n N}} \tag{14}$$

if $\Delta n^* = \rho$.

For

$N = 10^2$,	$R \approx 41.5$
$N = 10^3$,	$R \approx 33.9$
$N = 10^4$,	$R \approx 29.4$
$N = 10^6$,	$R \approx 24.0$
$N = 10^{12}$,	$R \approx 16.9$
$N = 10^{22}$,	$R \approx 12.5$

---

6 Some reduction can be achieved by separation of inner shell electron from the nuclear core.

This comparison shows that SF permits larger values of (α a μ) and is therefore less restrictive with respect to the nuclear and atomic requirements of the active medium than ASE as modeled by Tramell and Hannon.

Finally, if we remove the assumption that $\alpha >> 1$, a>>1 and $\mu > 0$, then the appropriate conditions for ASE and SF are

$$\mu (\alpha + 1) (a + 1) < \frac{\lambda^2 f}{2\pi} \frac{\Delta n^*}{21} \tag{15}$$

for ASE, and

$$\left(1 + \frac{\mu}{4}\right) (a + 1) (1 + \alpha) < \frac{3\lambda^2 f\rho}{4\pi\sqrt{2ln(N)}} \tag{16}$$

for SF.

III. PARAMETRIC FITS TO MONTE CARLO SIMULATIONS OF SUPERFLUORESCENCE

We have studied SF phenomena using Monte Carlo solutions (Ref. 4) of Maxwell-Bloch equations. The details of the calculations, which required a considerable amount of computer time, and our findings are described in two previous IDA reports (Refs. 4, 8). To save computer time in analyzing and predicting experimental results we have developed parametric models based on these Monte Carlo calculations.

Fig. III-1a shows the delay time normalized to τ_{SF} as a function of the cooperation number N. In the runs the attenuation coefficient $\mu = 0$, the dots represent Monte Carlo runs and the curve represents the least square fit to the parametric equation

$$\tau_D = a\,[1 + b \ln (N)]\ln(N), \tag{17}$$

in which the parameter values corresponding to the best fit are

$$a = 2.43 \quad ,$$

$$b = 0.02 \quad .$$

Figure III-1b shows a parametric fit to the same data in terms of $n = \ln N$, of the equation

$$\tau_D = \tau_{DO}\left[\,1+\beta_1 n+\beta_2 n^2\,\right], \tag{18}$$

in which the parameter values are:

$$\tau_{D0} = 0.158 \quad ,$$

$$\beta_1 = 67.885 \quad ,$$

$$\beta_2 = 7.067 \quad .$$

In their theoretical treatment Bonifacio and Lugiato (Ref. 9) [also cf. Gross and Haroche (Ref. 10)] obtained a logarithmic dependence on the cooperation number N, while Polder, Schuurmans, and Vrehen, in their work (Ref. 12) derived a dependence on the square of the logarithm of N. Our result, based on the work of Haake and Reibold (Ref. 13) is a linear combination of both.

N	τ_D
10^2	12.0
10^4	25.0
10^6	37.0
10^8	62.0
10^{10}	80.0
10^{12}	105.0
10^{14}	130.0
10^{16}	155.0

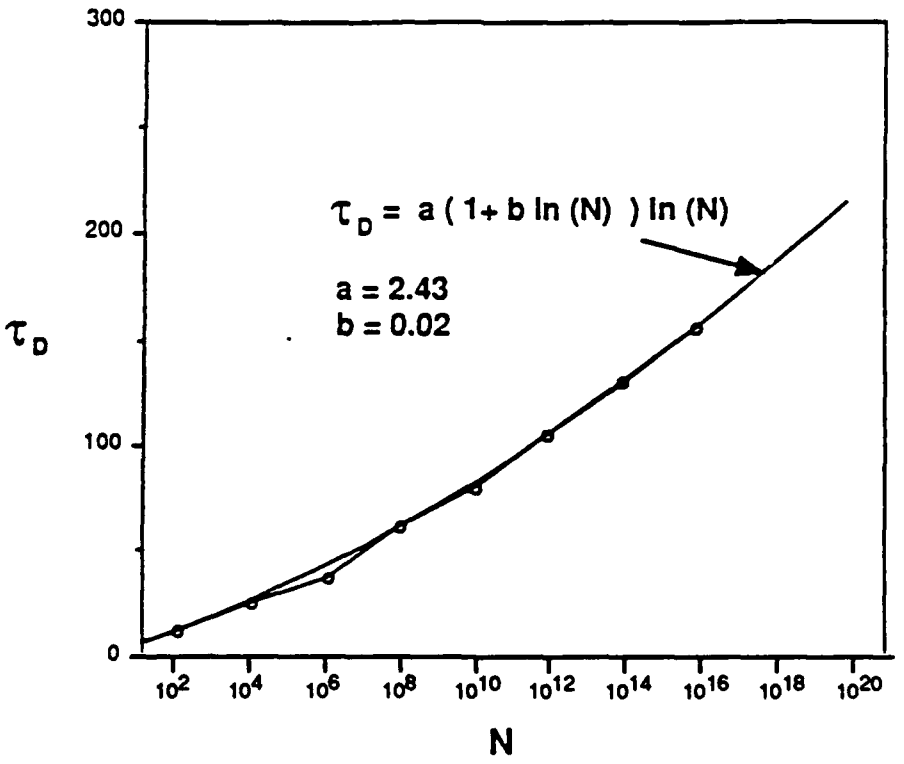

Figure III-1a. Parametric fit of delay time τ_D obtained from Monte Carlo runs as a function of N.

n	τ_D
4.6	12.0
9.2	25.0
13.8	37.0
18.4	62.0
23.0	80.0
27.6	105.0
32.2	130.0
36.8	155.0

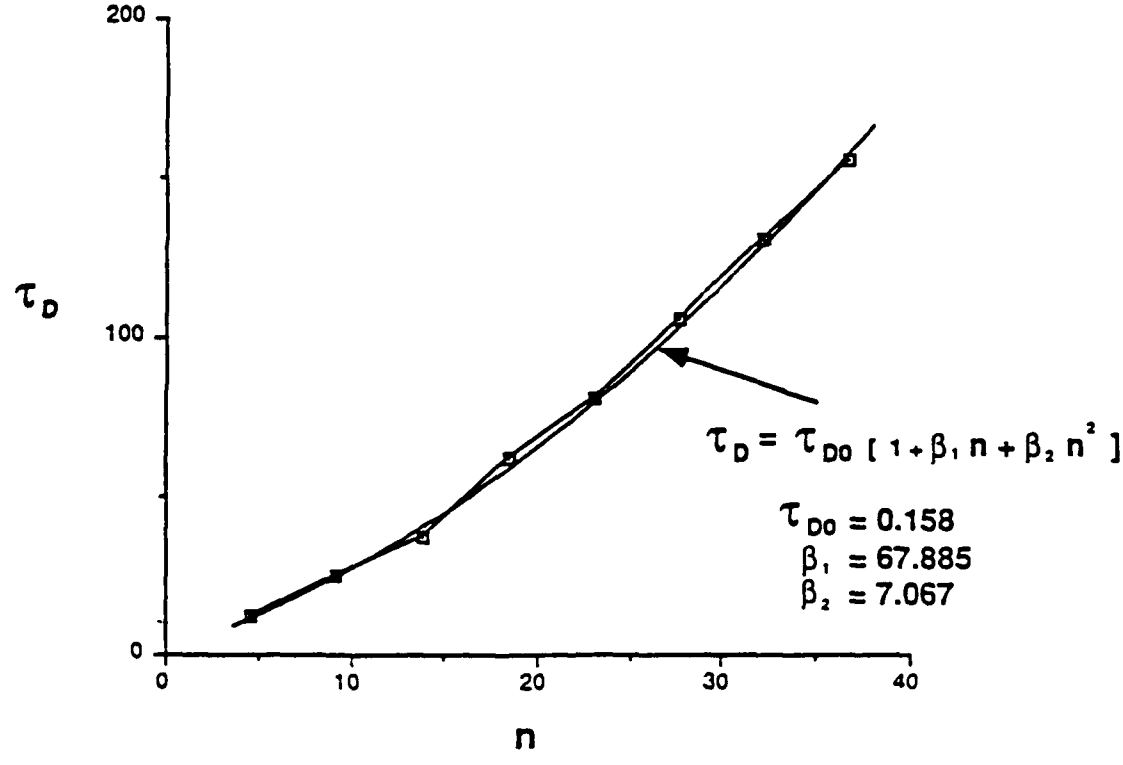

Figure III-1b. Parametric best fit to the delay time τ_D obtained from Monte Carlo runs as a function of n=/ n N.

We also ran Monte Carlo calculations for $N = 10^2, 10^3, 10^4$, and different values of μ. The time delay τ_D versus μ is plotted in Fig. III-2 for the different values of N. In Fig. III-3 we show the normalized area under the pulse as a function of μ. Note how closely the curves overlap, indicating little effect of the cooperation number on the change in total emission with attenuation. The effect of cooperation number on the delay time however is substantial. The results are summarized in Table III-1 which gives the pulse delay time, width intensity, and area under the pulse.

Figure III-4 (a, b, c) shows the parametric fit of the delay time τ_D as a function of the attenuation coefficient μ to the quadratic function

$$\tau_D = \left(\alpha + \beta\mu + \gamma\mu^2\right)\tau_o \quad . \tag{19}$$

The curve fit is for the calculated points that result in the curves in Fig. III-2. Table III-2 gives the corresponding parameters that define the quadratic fits.

It has been claimed (Refs. 1, 11) that a finite attenuation coefficient affects the development of SF pulses by restricting the active cooperating volume by limiting the cooperation length to $\frac{1}{\mu}$. We tested this assumption by comparing the delay time τ_{DMC} obtained from the Monte Carlo solution of the Maxwell-Bloch equations with the result, designated τ_{DV} for this purpose, obtained from Eq. (17) assuming $N \rightarrow \frac{N}{l\mu}$, or in normalized units of $\frac{t}{\tau_{SF}}$ and $\frac{x}{l}$,

$$\tau_{DV} = a\left[1 + b\ln\left(\frac{N}{\mu}\right)\right]\ln\left(\frac{N}{\mu}\right)\mu \quad . \tag{20}$$[1]

At $\mu = 1$, τ_{DV} from equation (17) for different N was normalized to the Monte Carlo result, τ_{DMC} (shown in Fig. III-2).

---

[1] τ_{DV} is in units of τ_{SF}, and the factor μ on the extreme right comes from the decrease of the cooperation number used in the definition of τ_{SF}.

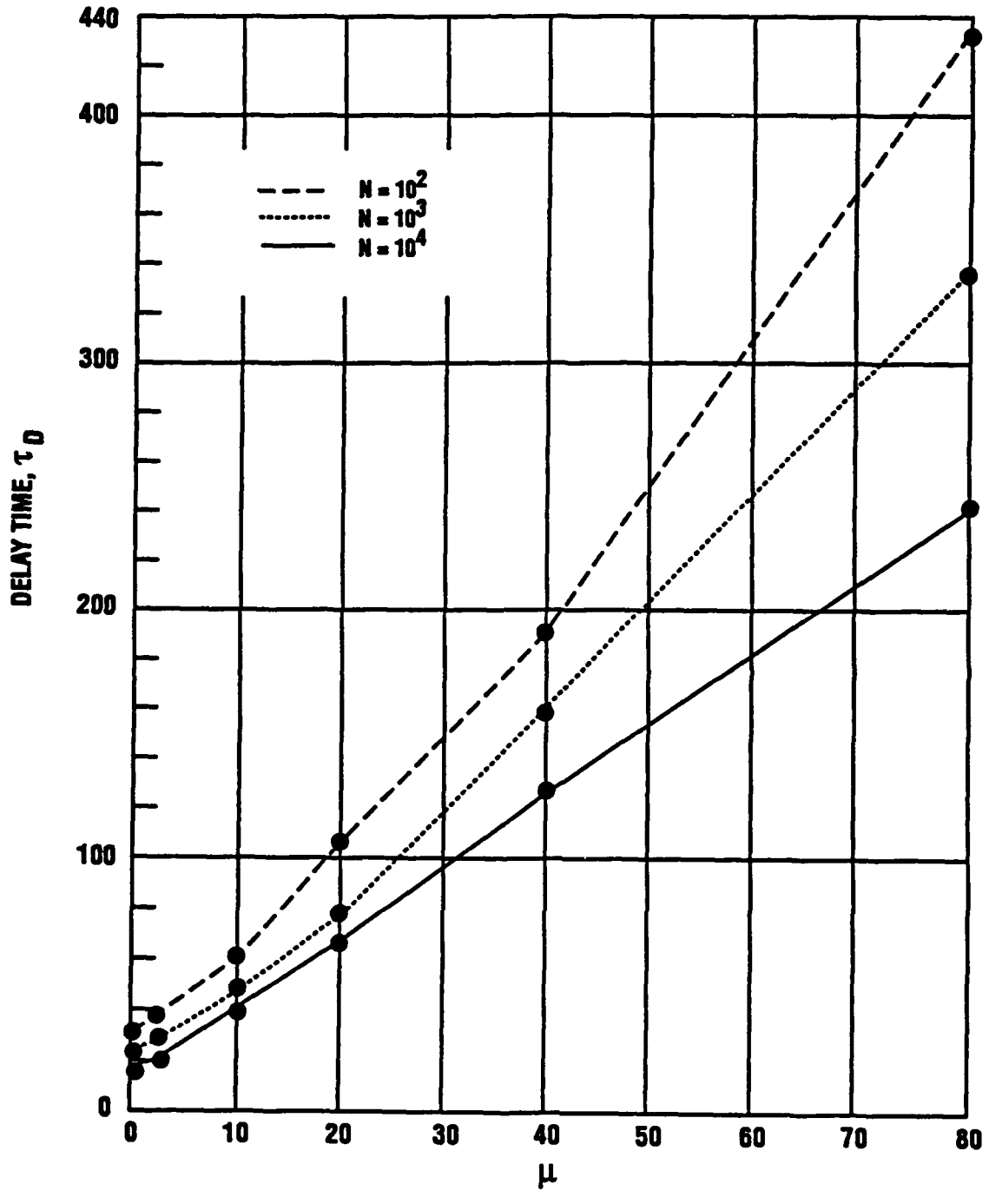

Figure III-2. SF Delay time τ_D as a function of linear attenuation coefficient μ. Points obtained from Monte Carlo calculation.

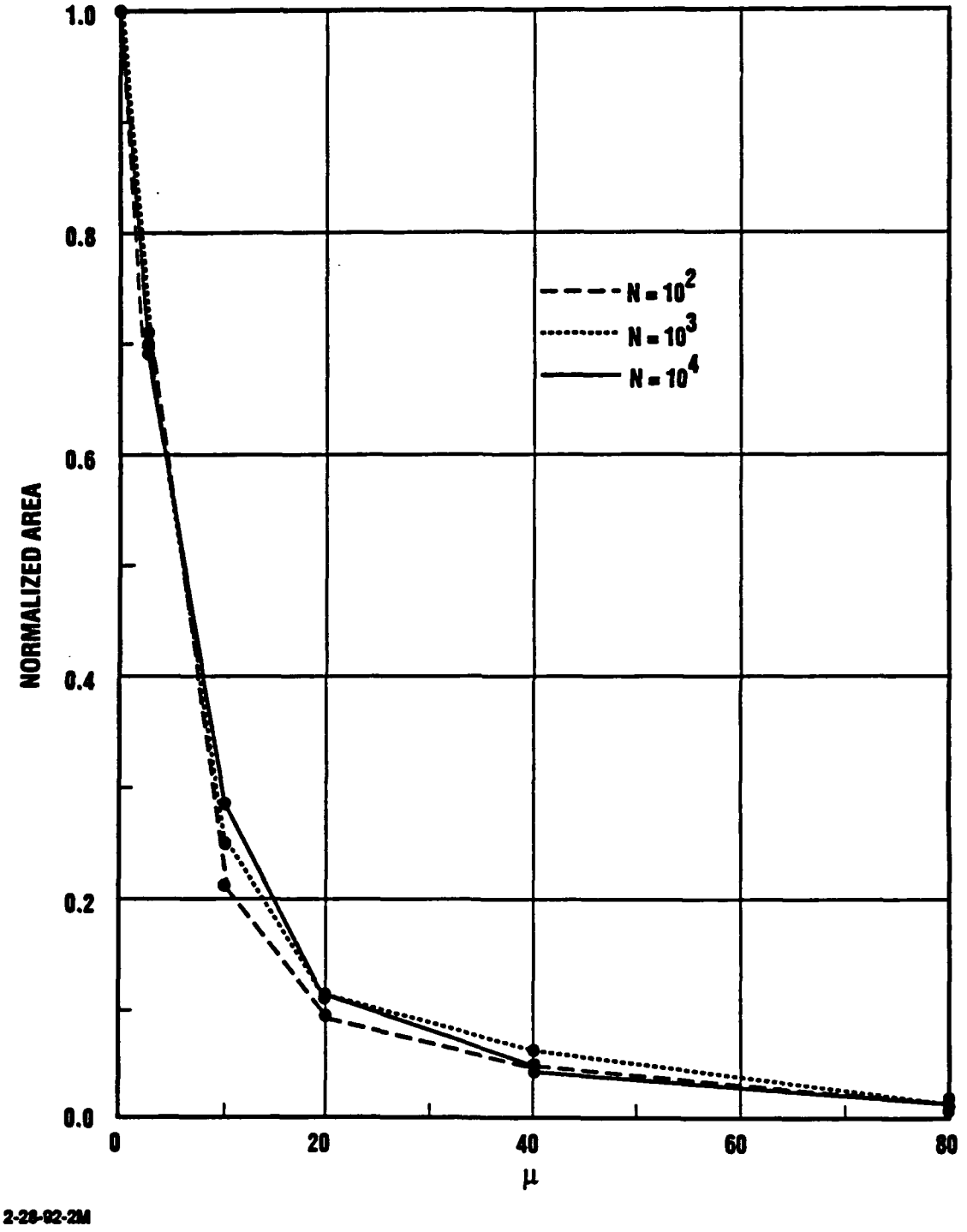

Figure III-3. Normalized area under SF pulses obtained from Monte Carlo calculation as a function of μ.

Table III-1. SF Pulse Characteristic Parameters

N	Attenuation Coefficient m	Delay Time t_D	Intensity	Pulse Width	Area Under Pulse	Normalized Area
10^2	0	17.5	0.0329	11.5	0.378	1.0
	2	20.0	0.0194	14.0	0.272	0.72
	10	38.0	0.00439	18.0	0.079	0.21
	20	67.0	0.00108	35.0	0.038	0.10
	40	125.0	0.000198	70.0	0.014	0.04
	80	240.0	0.0000385	156.0	0.006	0.016
10^3	0	23	0.0247	13.5	0.333	1.0
	2	27	0.0168	14.0	0.235	0.7
	10	47	0.00381	21.0	0.08	0.24
	20	77	0.00104	35.0	0.036	0.11
	40	155	0.000211	75.0	0.016	0.048
	80	338	0.0000231	180.0	0.00416	0.012
10^4	0	30	0.0189	16.0	0.302	1.0
	2	37	0.0126	16.5	0.208	0.69
	10	58	0.00353	42.0	0.085	0.28
	20	110	0.000991	33.0	0.033	0.11
	40	190	0.000181	64.0	0.0116	0.038
	80	430	0.000016	232.0	0.0037	0.012

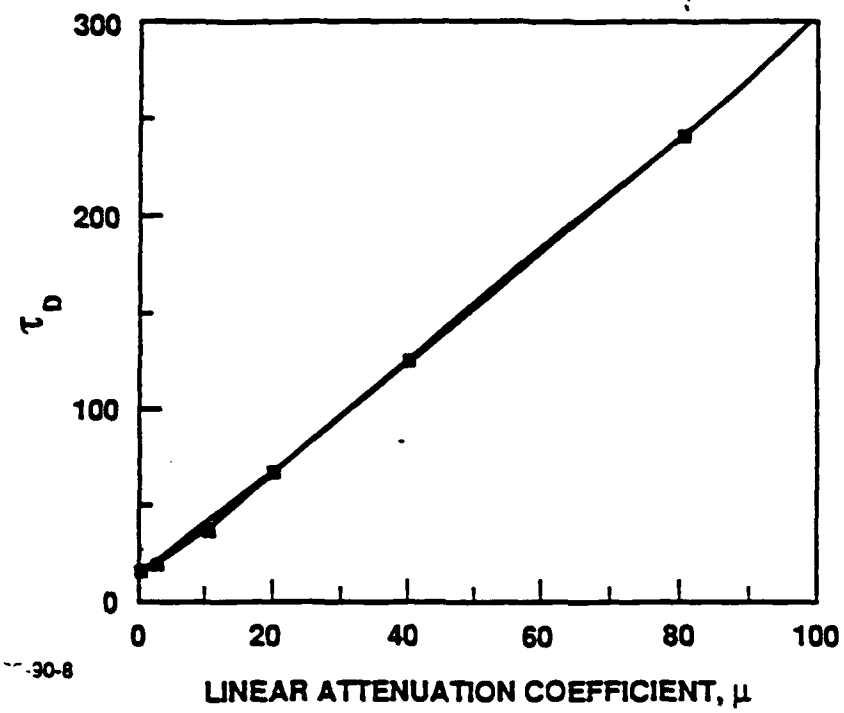

Figure III-4a. Parametric fit to data shown in Fig. IV-2 for N = 10^2. The best fit is given by $\tau_D = (1278+220\mu+1/4\mu^2)\ 1.17 \times 10^{-2}$.

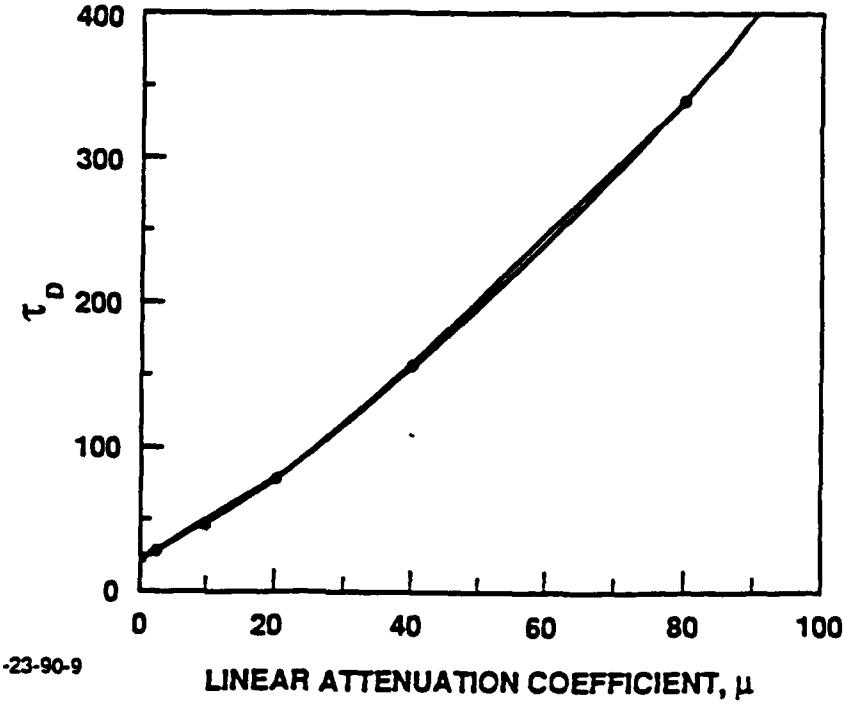

Figure III-4b. Parametric fit to data shown in Fig. IV-2 for N = 10^3. The best fit is given by $\tau_D = (307+37\mu+1/4\mu^2)\ 6.93 \times 10^{-2}$.

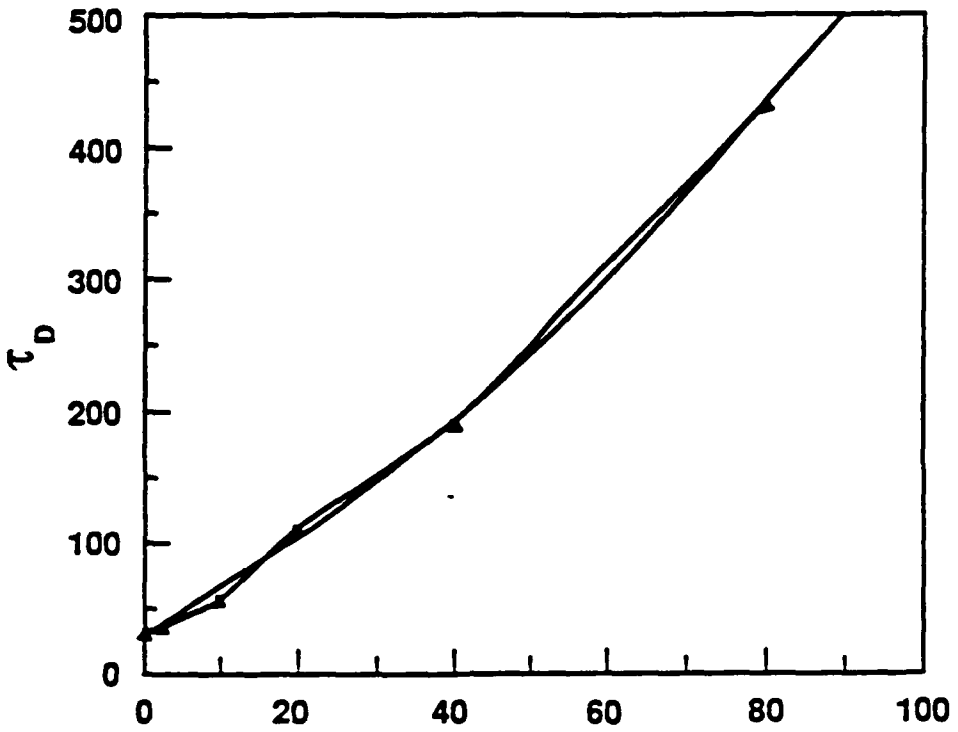

11-23-90-10

Figure III-4c. Parametric fit to data shown in Fig. IV-2 for N = 10^4. The best fit is given by $\tau_D = 9.1 \times 10^{-2}$ (327+35μ + 1/4 μ^2).

Table III-2. Parameters for Delay Time as a Function of Attenuation

N	α	β	γ	τ_o
10^2	1278.00	220.20	0.25	1.17×10^{-2}
10^3	306.89	37.25	0.25	6.93×10^{-2}
10^4	326.85	34.87	0.25	9.11×10^{-2}

The comparisons are shown in Fig. III-5(a-c) with the heavy line representing the Monte Carlo calculation τ_{DMC} and the dashed line the reduced volume result τ_{DV}. For N = 10^2 [Fig. III-5(a)], the two curves intersect at $\mu \sim 45$ and τ_{DV} approaches zero since $\frac{N}{\mu}$ approaches 1. Clearly the meaningful range of μ is $\mu < 20$ for N = 10^2. For higher N values this restriction occurs at higher μ values. The more interesting result of this comparison is that the volume restriction by μ which is the basis for the calculation of

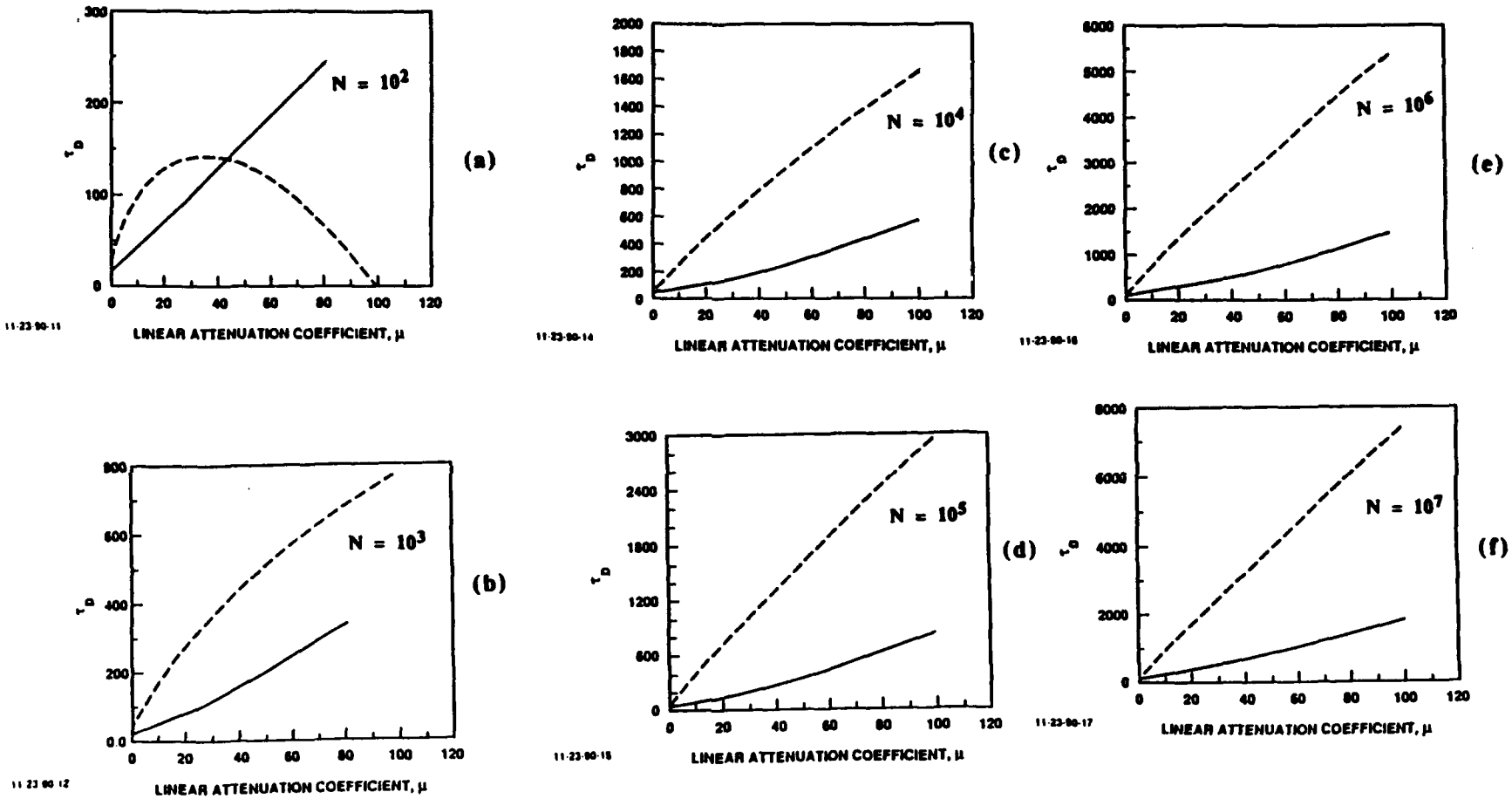

Figure III-5(a-f). A plot of SF delay times τ_{DV} and τ_{DMC} as a function of the linear attenuation coefficient μ. The delay time τ_{DV} (dashed line) was obtained from the reduced volume assumption [Eq. (2)] and τ_{DMC} (solid line) from the Monte Carlo simulations. The cooperation number N is 10^2 in (a), 10^3 in (b), 10^4 in (c), 10^5 in (d), 10^6 in (e), 10^7 in (F).

τ_{DV} gives a larger value for the delay time. If we assume that the Monte Carlo calculation is a better representation of the physical process and therefore represents the correct value, the volume reduction or restriction result τ_{DV} has to be modified. From the three figures showing the comparison between τ_{DV} and τ_{DMC}, we see that in the $\mu < 20$ range by reducing the attenuation coefficient μ by a factor of 3 an approximate value for τ_{DV} closer to τ_{DMC} can be obtained from Eq. 18. The factor increases for higher μ values, for example: at $N = 10^3$ and $\mu \sim 80$ the required factor to make the correction would be closer to 4.

IV. SUPERFLUORESCENCE IN ^{60}Co

A. CHARACTERISTIC PARAMETERS

In this section we apply the results of our earlier studies to examine the possibility of SF in ^{60}Co. We first determine the SF time τ_{SF} for ^{60}Co. We use this to generate delay time τ_D values (obtained from different theories) and we then check the SF condition $\sqrt{\tau_{SF}\,\tau_D} < \tau_\phi$ to determine the bound on the only free (unknown) parameter a, characterizing the inhomogeneous broadening.[1] Finally we check our preliminary results with the Maxwell-Bloch Monte Carlo calculations. The characteristic parameters are given in Table IV-1, and the partial energy diagram for ^{60}Co is shown in Fig. IV-1

Table IV-1. Characteristic Parameters for ^{60}Co

Parameter	Value	Symbol
Transition energy	58.6 ke V	E0
Wave length on resonance	0.2 Å (2×10^{-9}cm)	λ
Natural lifetime	628 sec.	τ_0
Recoilless fraction	0.304	f
Linear attenuation coefficient	12 cm^{-1}	μ
Internal conversion coefficient	48.3	α
Particle density (in solid form)	8.97×10^{22} cm^{-3}	ρ
Thermal neutron cross-section $^{59}Co + n \rightarrow {}^{60}Co$	20 barns	σ_n

[1] τ_ϕ is the dephasing time due to inhomogeneous broadening, etc.

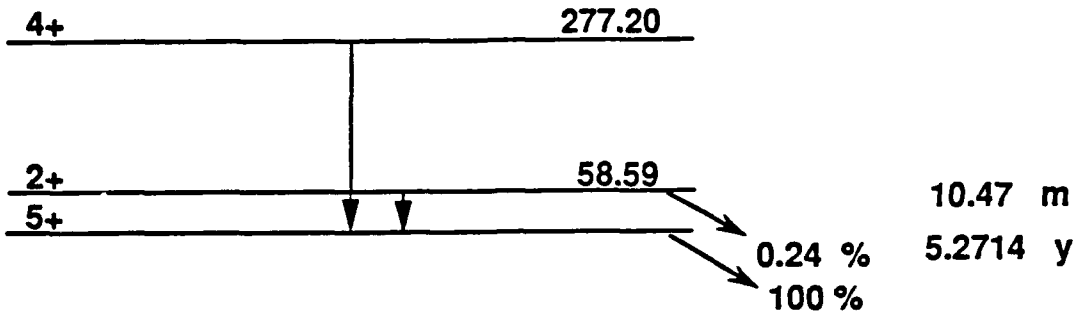

Figure IV-1. Level Structure of $^{60}CO_{27}$

The characteristic SF time, assuming an effective length limited by the attenuation coefficient and approximately $4/\mu$ (see Chapter III), is given by

$$\tau_{SF} = \frac{8\pi\,\tau_r}{3f\rho\lambda^2 l} = \frac{8\pi\,(1+\alpha)\,\tau_o}{3f\rho\lambda^2(4/\mu)} \quad ,$$

which for ^{60}Co gives $\tau_{SF} = 7.1$ sec. In units of τ_{SF} the lifetime is 88 and the natural decay rate $\Gamma = 1.1 \times 10^{-2}$.

The delay time has been derived in different developments with different dependences on the number of cooperating nuclei N. The number of cooperating nuclei is given by

$$N = \rho\lambda^2 l = 9 \times 10^4,$$

using a value of 0.25 cm for l. For the delay time, Bonifacio and Lugiato and Gross and Haroche use

$$\tau_D = \frac{1}{2}\tau_{SF}\,ln\,(N) \quad ; \tag{21}$$

on the other hand, Polder, Schuurmans, and Vrehen derived the expression

$$\hat{\tau}_D = \frac{1}{4}\tau_{SF}\left[ln\,(2\pi N)^{\frac{1}{2}}\right]^2 \tag{22}$$

for that quantity. They claim that the $ln^2(N)$ dependence is due to taking into account propagation effects that Bonifacio and Lugiato do not include in their model. From our Monte Carlo calculations in studies of the Maxwell-Bloch equations, including random sources and propagation effects, we found that

$$\bar{\tau}_D = a[1 + b\,ln\,(N)]\,ln\,(N) \tag{23}$$

with a = 2.43 and b = 0.02. These three results are compared in Fig. IV-2.

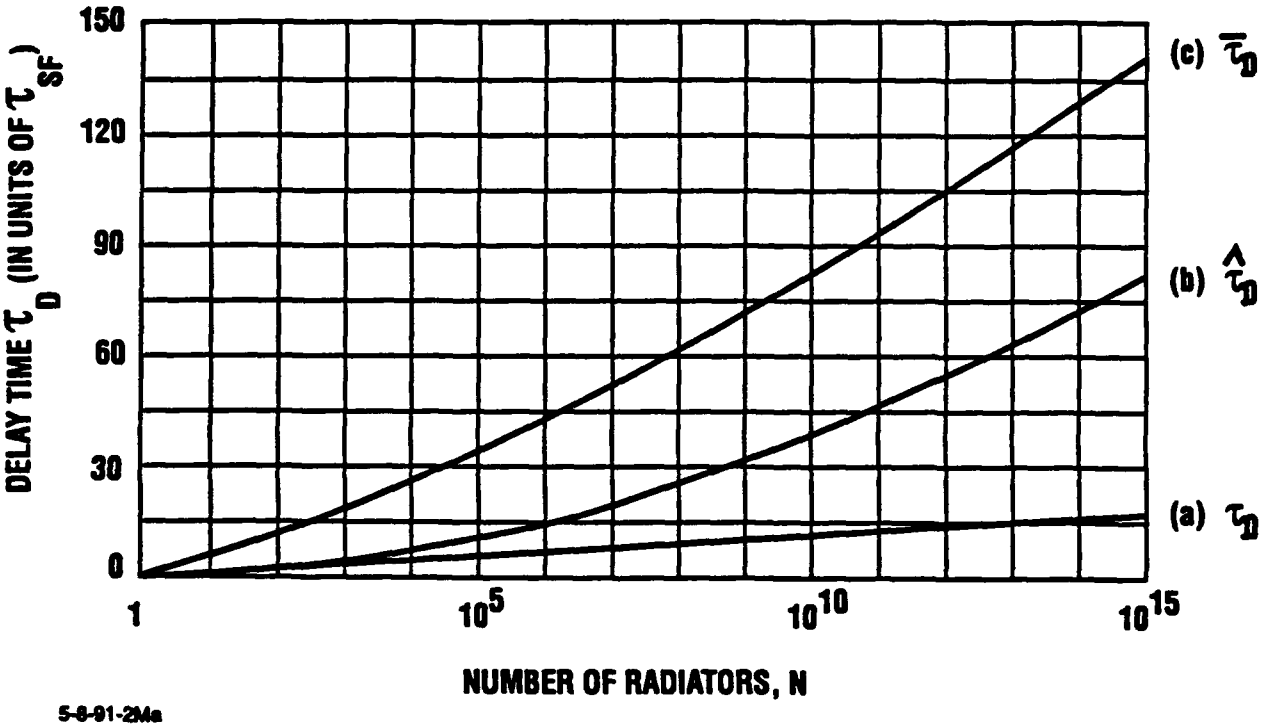

Figure IV-2. Comparison of Pulse Delay Times calculated from different theories as in (a) Bonifacio and Lugiato (Ref. 9) and Gross and Haroche (Ref. 10) results (τ_D of equation 8), (b) Polder, Schuurmans and Vrehen (Ref. 12) result ($\hat{\tau}_D$ of equation 9), (c) Haake and Reibold (Ref. 13) result ($\bar{\tau}_D$ of equation 10).

For Large N the effect of the $ln^2(N)$ term becomes important but for $N = 10^5$ this term contributes only about 20 percent of the $ln\,(N)$ term's contribution. Table IV-2 gives the values of $\frac{\tau_D}{\tau_{SF}}$, $\frac{\hat{\tau}_D}{\tau_{SF}}$ and $\frac{\bar{\tau}_D}{\tau_{SF}}$ for different values of N.

Table IV-2. Comparison of Pulse Delay Times calculated as a function of N

N	$ln(N)$	$\frac{\tau_D}{\tau_{SF}}$	$\frac{\bar{\tau}_D}{\tau_{SF}}$	$\frac{\hat{\tau}_D}{\tau_{SF}}$
10^2	4.6	2.3	12.2	2.6
10^3	6.9	3.4	19.1	4.8
10^4	9.2	4.6	26.5	7.6
10^5	11.5	5.8	34.4	11.1
10^6	13.8	6.9	42.8	15.3
10^7	16.1	8.0	51.8	20.1
10^8	18.4	9.2	61.2	25.6

B. BOUNDING CALCULATION

Using $\tau_{SF} = 7.1$ sec, we generate τ_D and $\bar{\tau}_D$ for ^{60}Co for different values of N shown in Table IV-3.

Table IV-3. *Delay Times Calculated two different ways*

N	τD(sec)	$\bar{\tau}_D$(sec)
10^2	16.3	86.6
10^3	24.1	135.6
10^4	32.7	188.2
10^5	40.8	244.2
10^6	49.0	303.9
10^7	56.8	367.8
10^8	65.3	434.5

All of the calculated delay times are smaller than the natural lifetime (628 sec), and so in the absence of attenuation and dephasing (inhomogeneous broadening) an inverted population of ^{60}Co should produce SF pulses. We still have to include these effects for a more realistic estimate and this will be done in the next section.

A relationship exists that allows us to put an upper bound on the inhomogeneous broadening parameter in terms of μ and α, which are known (Table IV-1). In the approximation using the τ_D derived by means of semiclassical or mean field theory for the delay time we have [from Eq. (16), Chapter II]

$$\left(\frac{\mu}{4}+1\right)(\alpha+1)(a+1) < \frac{3\lambda^2 \rho}{4\pi\sqrt{2ln(N)}} \quad ,$$

which with $\alpha = 48.3$ and $\mu = 12$ and $N = 10^5$ gives $a < 27$ (for $N = 10^3$, $a < 35$) as the requirement on inhomogeneous broadening in order to achieve SF. When we use $\bar{\tau}_D$ in the estimation the requirement becomes $a < 10$ for $N = 10^5$ and $a < 14$ for 10^3. A similar calculation for ASE in ^{60}Co gives $a < 1.4$ as the requirement on inhomogeneous broadening.

In the directions of the crystal where the Borrmann effect reduces the attenuation to $\mu \approx 0$ the requirement for SF is $a < 112$ for $N = 10^5$ when τ_D is used in the estimate. All of these estimates depend on full inversion at $t = 0$. To include finite inversion times and treat all of the pertinent parameters in a consistent way we require the solution of the Maxwell-Bloch equations as described in Refs. 4 and 8. This will be discussed in the next section. As a final summary of the bounding study, we present curves that bound the values μ and a for different cooperation numbers N.

Figures IV-3(a, b) give the SF conditions according to bounds determined by Eq. (16). For each curve representing a particular value of nuclear density ρ the area below and to the right gives the acceptable values of a and μ. Figure IV-4 gives the corresponding results for ASE according to bounds determined by Eq. (15). Figure IV-4 for ASE is drawn to the same scale as the SF curves in IV-3 (a, b). Note the restricted parameter space for ASE as compared to SF.

C. MAXWELL-BLOCH RESULTS

The interplay of the important physical parameters in dynamical full-time dependent treatment of the physical phenomena is needed for a realistic assessment of the feasibility of SF. In this section we present our results on the SF pulse emission in ^{60}Co from the Maxwell-Bloch Monte Carlo calculations. Using parameters given in Table IV-1 as the nominal values, we examined the possibility of SF by studying the pulse as a function of the inhomogeneous broadening parameter a, and attenuation coefficient μ. Some SF pulses

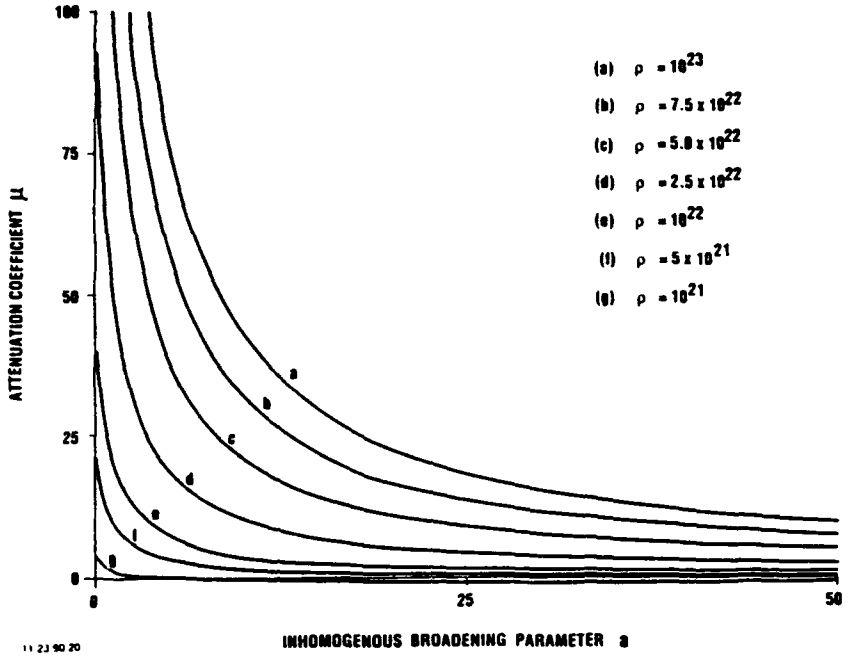

Figure IV-3a. A plot of μ versus a for SF at the boundary. Each curve is calculated for a particular value of the density ρ as marked and with $N = 10^3$. All the points in the region to the left of the curve give the acceptable values of a and μ for SF.

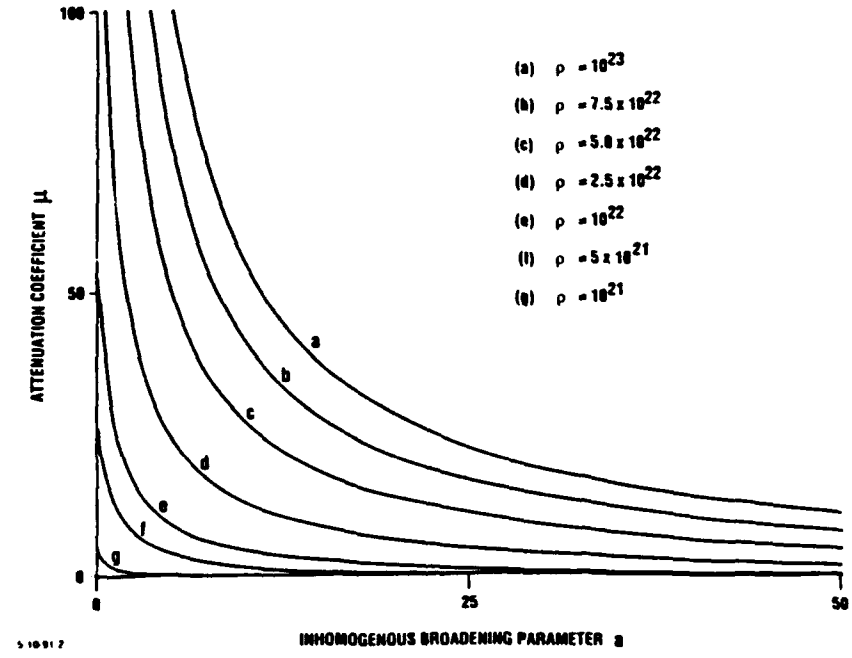

Figure IV-3b. A plot of μ versus a for SF at the boundary. Each curve is calculated for a particular value of the density ρ as marked and with $N \approx 10^2$. All the points in the region to the left of the curve give the acceptable values of a and μ for SF.

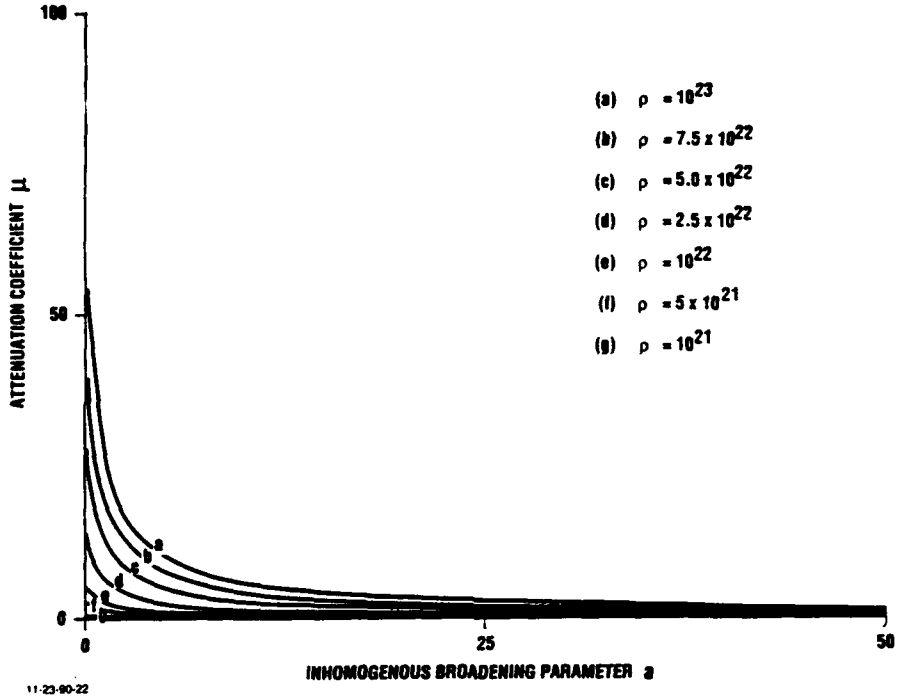

Figure IV-4. A plot of μ versus a for ASE at the boundary. Each curve is calculated for a particular value of the density ρ as marked. All the points in the region to the left of the curve give the acceptable values of a and μ for ASE.

calculated for ^{60}Co with the Maxwell-Bloch equations described in Ref. 8 are shown in Fig. IV-5, IV-6 and IV-7. Pulse peak intensity I_o, delay time τ_D (in seconds), and the integrated pulse intensity per nucleus, for the different values of parameters μ, the attenuation coefficient (in cm^{-1}), and a, the inhomogeneous broadening parameter, are given in Table IV-4. For these calculations we assumed l = 1 cm, giving $N = \rho\lambda^2 l = 1.1 \times 10^5$ and, from Eq. (2), $\tau_{SF} = 2.4$ seconds. Optimizing for the geometrical divergence and the diffraction limits on a cylindrical active region of length l and diameter d, requires $d=\sqrt{l\lambda}$. For l = 1 cm and $\lambda = 2.0 \times 10^{-9}$cm, we get $d \simeq 4.5 \times 10^{-5}$ cm and a beam divergence of $\theta_D = 9 \times 10^{-5}$ radians.

The possibility of observing nuclear SF is considered by comparing the SF emission as characterized in Table IV-4 with the spontaneous emission from the natural decay of ^{60}Co. The two experimental techniques considered, A and B, are shown in Fig. IV-8. In experiment A, a sample composed of small single crystals of ^{60}Co, randomly oriented, is placed in a thermal neutron reactor and the population inverted. The sample is then placed in a 4π detector and the count as a function of time measured.

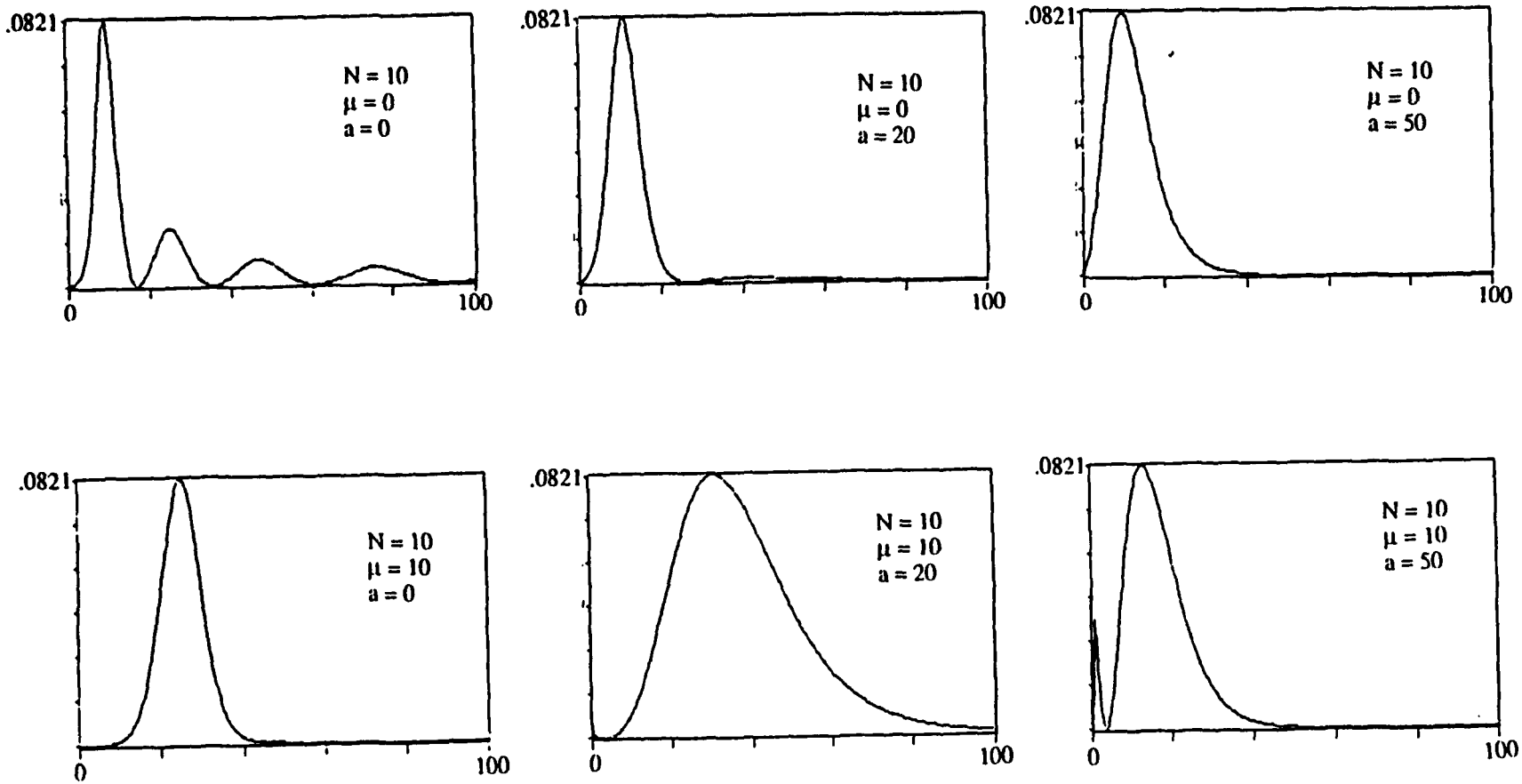

Figure IV-5. SF pulses calculated with the Maxwell-Bloch equations in a Monte Carlo simulation of the vacuum fluctuations. The parameters are $\gamma = 10$, $\Gamma_2 = 10^{-6}$, $\Gamma_3 = 3.75 \times 10^{-3}$ and N, μ and a as indicated in the figure.

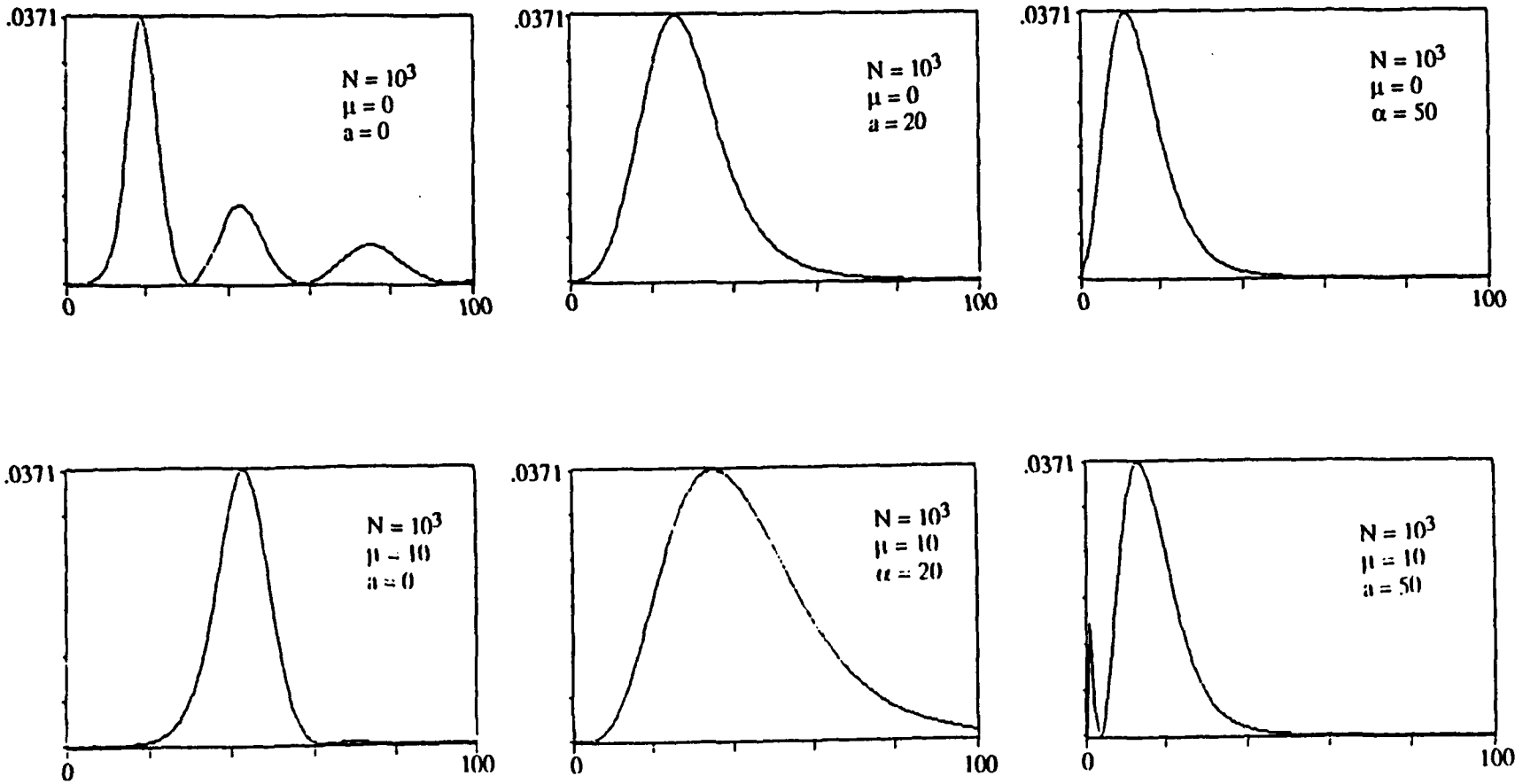

Figure IV-6. SF pulses calculated with the Maxwell-Bloch equations in a Monte Carlo simulation of the vacuum fluctuations. The parameters are $\gamma = 10$, $\Gamma_2 = 10^{-6}$, $\Gamma_3 = 3.75 \times 10^{-3}$ and N, μ and a as indicated in the figure.

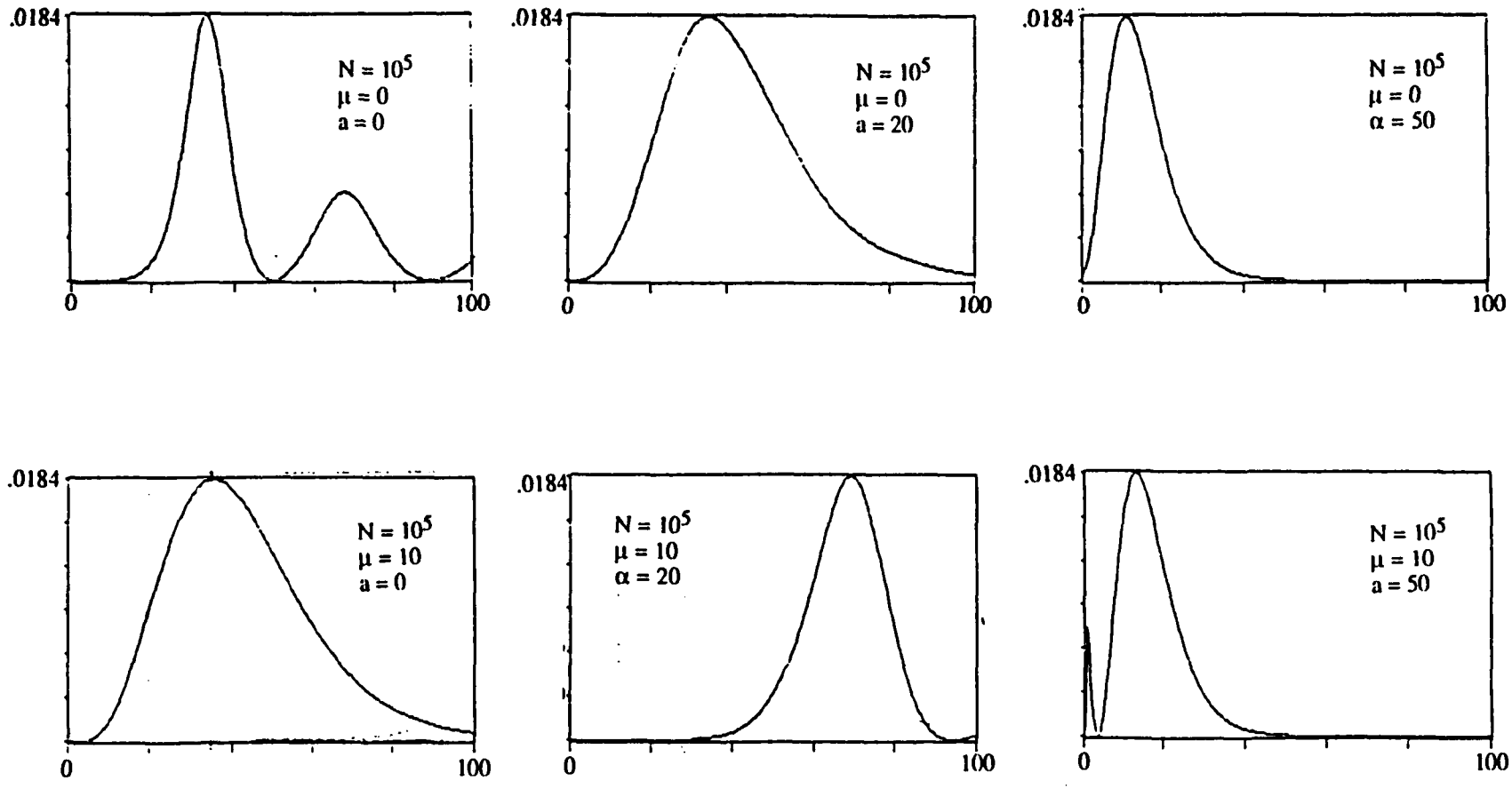

Figure IV-7. SF pulses calculated with the Maxwell-Bloch equations in a Monte Carlo simulation of the vacuum fluctuations. The parameters are $\gamma = 10$, $\Gamma_2 = 10^{-6}$, $\Gamma_3 = 3.75 \times 10^{-3}$ and N, μ and a as indicated in the figure.

Table IV-4. SF Pulse Parameters calculated for ^{60}CO from the Maxwell-Bloch equations. Shown are the SF pulse delay time τ_D, normalized pulse intensity (photons/second)/N in parenthesis ( ) and integrated normalized intensity ($^{photons}/_{N}$) in brackets [ ] for different values of the attenuation μ (cm^{-1}) and inhomogeneous broadening a, assuming $N = 1.1 \times 10^5$ cooperating nuclei and a pumping rate of 4.2 s^{-1}.

μ \ a	0	5	10	20	50
0	119 (0.018) [0.348]	136 (0.076 [0.163]	167 (2×10^{-4}) [0.0703]	122 (5.47×10^{-5}) $[2.17 \times 10^{-3}]$	48 (5.96×10^{-2}) $[1.0 \times 10^{-5}]$
6	190 (0.0055) [0.118]	221 (1×10^{-4}) [0.0376]	252 (4.1×10^{-5}) $[2.75 \times 10^{-3}]$	133 (4.77×10^{-7}) $[1.95 \times 10^{-5}]$	48 (5.16×10^{-9}) $[8.62 \times 10^{-8}]$
12	269 (0.0017) [0.0417]	381 (3.85×10^{-5}) $[3.38 \times 10^{-3}]$	252 (4.41×10^{-7}) $[3.18 \times 10^{-5}]$	129 (5.08×10^{-9}) $[2.07 \times 10^{-7}]$	3 (5.89×10^{-10}) $[1.02 \times 10^{-8}]$

Figure IV-8. Two experimental setups for detecting nuclear SF. In experiment A, a polycrystalline sample is used and both SF and NSD give isotropic radiation distributions; while in experiment B an acicular geometry provides a highly directional SF beam.

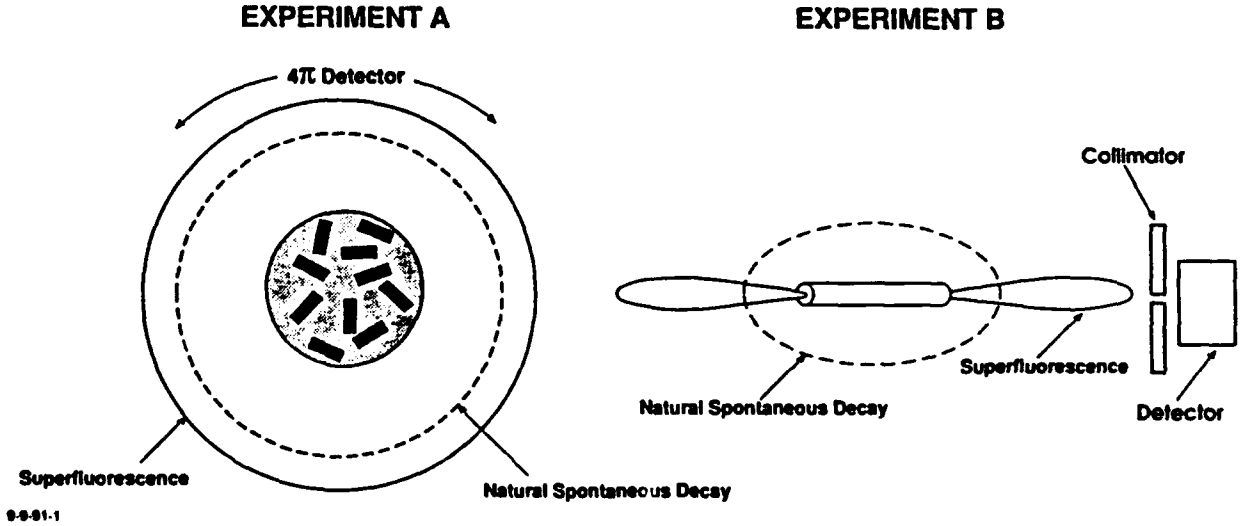

No attempt is made at angular discrimination of the SF emission from the natural decay and only the measurement of the emission rate is used to detect SF. In experiment B the sample is prepared in a cylindrical geometry, irradiated and placed in front of a collimator so that the directional beam characteristics can be used to discriminate against the natural decay. The ratio of the photon count from SF pulses divided by the spontaneously emitted photons in the natural decay process integrated over all angles (detected in a 4π detector) is 2.9 when $a = 0$, $\mu = 0$ (case 1); 1.0×10^{-4} when $a = 50$ and $\mu = 0$ (case 2); and 8.6×10^{-6} when $a = 20$, $\mu = 12$ (case 3). We also lowered the pumping rate to $\gamma = 10^{-5}$ (equivalent to $2.1 \times 10^{+17}$ neutrons/cm^2) and repeated the $a = 0$, $\mu = 0$ calculation (case 4) with the result 1.6×10^{-8}. If advantage is taken of the directionality of the SF pulse in the experimental design then the small divergence of the SF beam compared to the isotropic distribution of the natural decay would permit discrimination and reduction of the effect of the natural decay, in the axial direction as compared to the SF pulse, by a factor of $\frac{\theta_D^2}{4\pi} = 2.0 \times 10^{-10}$. The photon count from the SF pulse compared to the natural decay would increase to 1.5×10^9 for $a = 0$, $\mu = 0$ (case 1), 4.9×10^5 for $a = 50$, $\mu = 0$ (case 2), and 4.2×10^3 for $a = 20$ and $\mu = 12$ (case 3). For case 4 we obtained 25 as the ratio of SF to natural photons. These results are tabulated in Table IV-5. In summary, for a Borrmann direction along the propagation axis (case 1), SF could be detected on the basis of time development of the decay, and no discrimination based on angular distribution is necessary. In case 2, again along the Borrmann direction but now with inhomogeneous broadening of $a = 50$, angular discrimination would have to be used to detect the SF. In case 3, without the Borrmann effect present and with inhomogeneous broadening of $a = 20$, the SF could also be observed with the help of angular discrimination obtained through collimation. In case 4, with the reduced pumping rate, both the Borrmann effect and reduced inhomogenous broadening are required for the observation of SF.

Figures IV-9 and IV-10 show calculated pulse shapes in the presence of natural decay for case 1 without assuming angular discrimination, and case 2 with angular discrimination of only $\theta = 10^{-2}$ radians more easily available experimentally instead of the lower limit permitted by the divergence of the SF beam of $\theta_D = 9 \times 10^{-5}$. In both figures, (a) shows separately the photon intensity calculated for both processes and (b) the sum of the intensity of the two processes.

Table IV-5. Predictions for ^{60}Co Experiments

		Total Count Ratio N_{SF}/N_{NSD}	
		Experiment A	Experiment B
		polycrystal whisker	single crystal
Case 1	$\gamma = 10$ $a = 0$ $\mu = 0$	2.9	4.5×10^{9}
Case 2	$\gamma = 10$ $\mu = 0$ $a = 50$	10×10^{-4}	1.5×10^{5}
Case 3	$\gamma = 10$ $\mu = 12$ $a = 0$	8.4×10^{-6}	1.3×10^{3}
Case 4	$\gamma = 10^{-5}$ $\mu = 0$ $a = 0$	1.3×10^{-7}	2.1×10^{2}

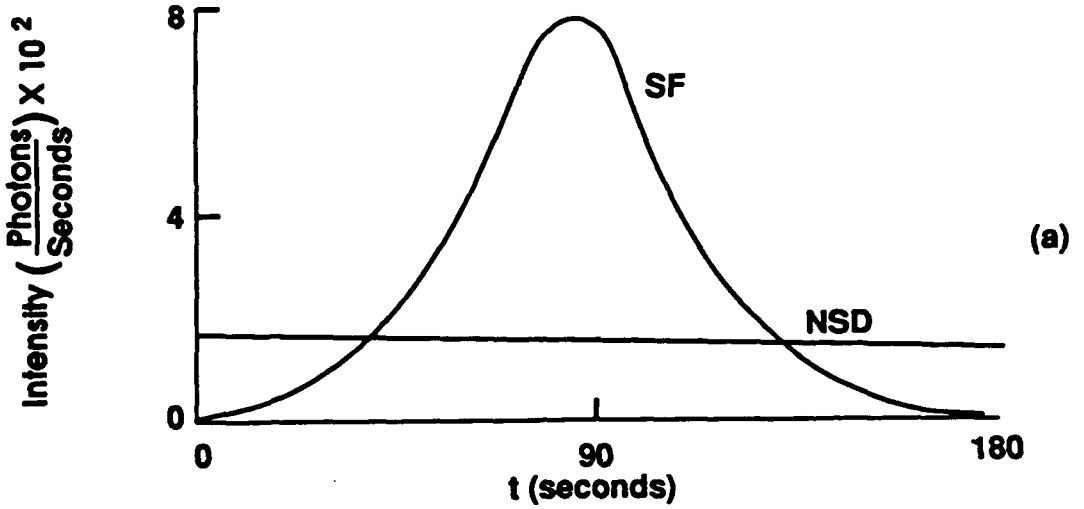

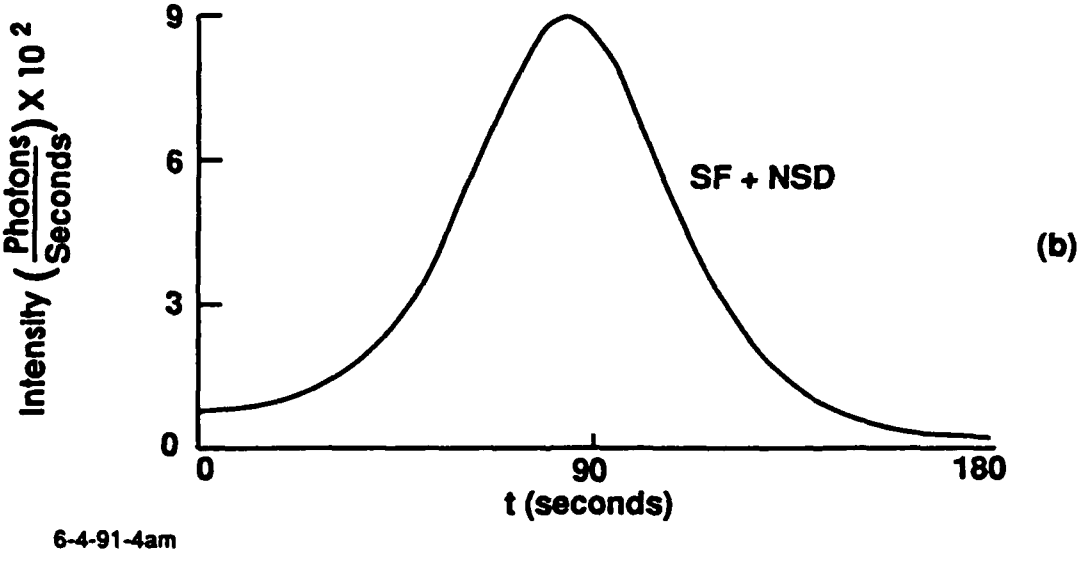

Figure IV-9. SF and Natural Spontaneous Decay (NSD) in ^{60}Co Assuming no attenuation (μ = 0), no inhomogeneous broadening (a = 0), and no Directional Discrimination. The scale is linear for both axes. The intensity is given in photons per second per emitter.

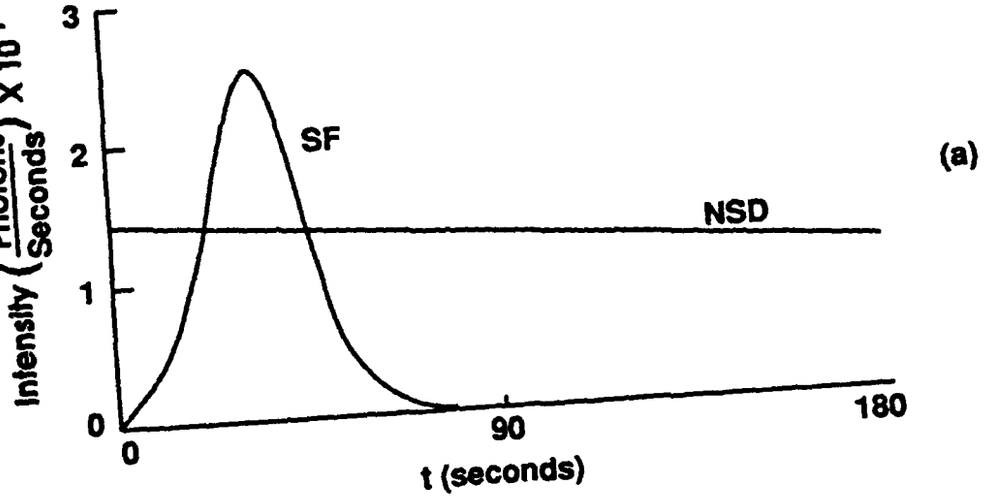

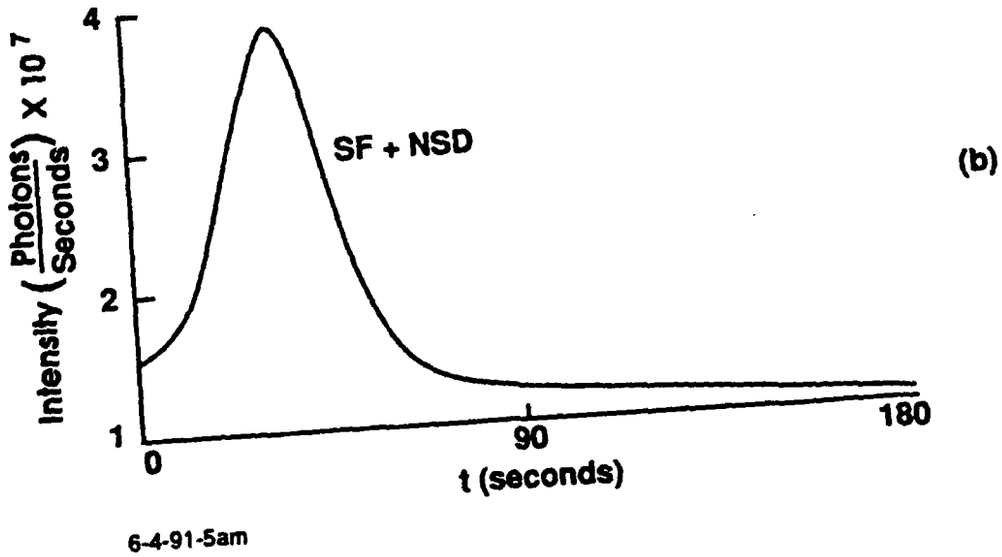

Figure IV-10. Directional Discrimination of SF Over Natural Decay. SF and Natural Spontaneous Decay (NSD) in ^{60}Co was Calculated Assuming Measurement Along the Axis of a Cylindrical Active Region, Inhomogeneous Broadening Present with a = 50 and Borrmann Effect Along the Axis, $\mu = 0$. The scale is linear for both axes. The intensity is given in photons per second per emitter.

We now have to project the results of our calculations onto the real world situation and consider the experimental realization of our predictions for observing SF in ^{60}Co. The calculations leading to the results shown in Table IV-4 assumed a pumping rate in normalized units of $\gamma = 10$. This corresponds to a thermal neutron flux of $J = 2.1 \times 10^{23}$ $cm^{-2}S^{-1}$ which can certainly be obtained as a result of nuclear explosions (Ref. 14), but is out of reach of available continuously operating reactors. Table IV-6 shows the calculated degradation of the SF pulse intensity as the pumping rate decreases. The lower pumping rates with $\gamma = 10^{-4}$, 10^{-5} require fluxes that were considered within reach of practical reactor designs in 1975, and so should be at least physically attainable from the point of view of reactor designers.

Table IV-6. Total Integrated Intensity of SF pulses as a function of pumping rate.

Pumping Rate	Neutron Flux	Integrated Intensity/N		
$\gamma (I/\tau_{SF})$	$J (cm^{-2} \cdot s^{-1})$	Case 1 $\mu = 0, a = 0$	Case 2 $\mu = 0, a = 50$	Case 3 $\mu = 12, a = 20$
10	2.1×10^{23}	0.348	1.1×10^{-5}	2.0×10^{-7}
1.0	2.1×10^{22}	0.348	6.5×10^{-6}	6.7×10^{-8}
0.1	2.1×10^{21}	0.264	8.3×10^{-8}	5.0×10^{-8}
0.01	2.1×10^{20}	0.146	3.1×10^{-9}	7.2×10^{-9}
0.002	4.2×10^{19}	8.95×10^{-3}	7.1×10^{-10}	1.4×10^{-9}
0.001	2.1×10^{19}	5.1×10^{-4}	-	-
0.0001	2.1×10^{18}	13×10^{-7}	-	-
0.00001	2.1×10^{17}	1.6×10^{-8}	-	-

The Borrmann effect has been observed and predictions indicate that suppression of attenuation by two orders of magnitude is certainly possible under the right conditions (Ref. 15). Inhomogeneous broadening has been discussed in the literature, and theoretical predictions using a static nuclear dipole-dipole interaction model give a value of $a = 10^5$ for this isomer (Ref. 16). Subsequent measurements by three different groups (Refs. 17-19) of self attenuation in a ^{109}Ag source gave $a \approx 30$-50. In addition to this, relaxation was proposed as a possible mechanism (Ref. 19) to explain the discrepency between these

measurements and the calculated value of 10^5 from the static dipole-dipole interaction (Ref. 16). We discuss the effect of relaxation on SF in another publication (Ref. 8).

D. CONCLUSIONS

This paper considers a generalized version of the Haake-Reibold model of superfluorescence in a multilevel system of emitters, having up to four energy levels. The generalized version takes into account finite pumping rates, spatial attenuation of the electromagnetic field, dephasing, and population depletion due to processes such as internal conversion and spontaneous, but noncollective, transverse emission.

In this paper we study the dependence of emitted pulse shapes on the statistics and time dependence of the noise sources. Monte Carlo results obtained by averaging 25 to 100 pulses, which seem to be adequate samples, also depend upon the noise source variance.

We find that the spatial attenuation parameter μ reduces the pulse peak and shifts it to longer times. The peak will decrease gradually but will not disappear if dephasing mechanisms that reduce the macroscopic dipole, built up by the noise source, do not exist and population depletion mechanisms do not destroy the inversion.

Small values of the dephasing factor have no effect on the emitted pulse delay time or intensity, but when the dephasing rate due to either homogeneous or inhomogeneous broadening is comparable to the superfluorescence decay rate, $1/\tau_{SF}$, the delay time starts to increase with increasing values of the dephasing factor until it reaches a maximum, after which it decreases rapidly. Consistently, the inhomogeneous effect is stronger than the homogeneous effect for the same amount of broadening.

Because of spatial attenuation, for maximum intensity of the pulse radiated out of the active region, the choice of the region's length should be governed by the values of the attenuation factor μ and the coupling constant g_1 associated with coupling between the emitters and the electromagnetic field. The optimum length will depend on details of the propagating electromagnetic field inside the active region.

The theory developed in this paper is applied to the 58 keV transition in ^{60}Co. It is found that for sufficiently intense pumping with thermal neutrons an inversion in ^{60}Co can be achieved and a SF pulse detected experimentally.

REFERENCES

1. G.T. Trammell and J.P. Hannon, "Threshold Conditions for Pulsed Gamma Ray Lasers," *Optics Comm.*, Vol. 15, No. 3, 1975, pp. 325-329.

2. G.C. Baldwin,"Two-Step Pumping of a Superradiant Graser," in *Proceedings of the IST/IDA Gamma-Ray Laser Workshop*, B. Balko et al., eds., IDA Memorandum Report M-162, 1986, pp. 216-254.

3a. J. Okada, K. Ikeda, and M. Matsuoka, *Optics Comm.*, Vol. 27, 1978, p. 321.

b. M.S. Malcuit, I. J. Maki, D.J. Simkin, and R.W. Boyd, *Phys. Rev. Lett.* 59 (11), 1189, 14 September 1987.

4. B. Balko, *IDA Gamma-Ray Laser Annual Summary Report (1988)--Investigation of the Feasibility of Developing a Laser Using Nuclear Transitions*, IDA Paper P-2175.

5. M.F.H. Schuurmans, "Superfluorescence and Amplified Spontaneous Emission in an Inhomogeneously Broadened Medium," *Optics Comm.*, Vol. 34, No. 2, 1980, pp. 185-189.

6. F.T. Arrechi and E. Courtens, "Cooperative Phenomena in Resonant Electromagnetic Propagation," *Phys. Rev. A*, Vol. 2, No. 5, 1970, pp. 1730-1737.

7. J.H. Eberly, "Inhomogenous Broadening in the Theory of Superradiant Emission," *Acta Physica Polonica*, Vol. A39, 1971, pp. 633-638.

8. B. Balko, I.W. Kay, and J. Neuberger, *IDA Gamma-Ray Laser Annual Summary Report (1989)--Investigation of the Feasibility of Developing a Laser Using Nuclear Transitions*, IDA Paper P-2335.

9. R. Bonifacio and L.A. Lugiato, "Cooperative Radiation Processes in Two-Level Systems: Superfluorescence," *Phys. Rev. A*, Vol. 11, No. 5, 1975, pp. 1507-1521.

10. M. Gross and S. Haroche, *Superradiance: an Essay on the Theory of Collective Spontaneous Emission*, North-Holland Pub. Co., Amsterdam, 1982.

11. G.C. Baldwin and M.S. Feld, *J. Appl. Phys.*, Vol. 59, 1986, pp. 3665.

12. D. Polder, M.F.H. Schuurmans, and Q.H.F. Vrehen, *J. Opt. Soc. Am.*, Vol. 68, 1978, pp. 699.

13. F. Haake and R. Reibold, "Interplay of Superfluorescence and Incoherent Processes in Multilevel Systems," *Phys. Rev. A*, Vol. 29, No. 6, 1984, pp. 3208-3217.

14. J.C. Solem, LASL Report LA-7898-MS(1979).

15. J.P. Hannon and G.T. Trammell, *Optics Comm.*, Vol. 15, No. 3, 1975, p 330.

16. G.E. Bizina, A.G. Beda, N.A. Burgov, and H.V. Davidov, *Sov. Physics JETP* 18, 1964, p. 973.

17. W. Wildner and U. Gonser, *J. Physics. Coll.* C2 Suppl., No. 3, 40, 1979, p. C2.

18. G.R. Hoy, S. Rezaie-Serej, R.D. Taylor, *Hyperfine Interactions*, Vol. 58, 1990, p. 2513.

19. P. Boolchand and R. Coussement (unpublished).

20. G. S'heeren, M. Van Den Bergh, R. Coussement, R.N. Enzweiler, R. Harris, Y. Wu, P. Boolchand, R.D. Taylor, M. Cyamukungu, J. Lehmann, and L. Grenacs, *Proceedings of International Conference on Lasers '90.*

APPENDIX A

THE TRAMMELL-HANNON MODEL OF AMPLIFIED SPONTANEOUS EMISSION (ASE)

APPENDIX A
THE TRAMMELL-HANNON MODEL OF AMPLIFIED SPONTANEOUS EMISSION (ASE)

In this appendix we discuss pulse propagation through an amplification medium, calculate pulse shapes as a function of gain and attenuation, and consider the appropriate form of the threshold conditions for pulse amplification. Our calculations are based on the Trammell and Hannon (Ref. A-1) model of ASE which has certain severe limitations. In this appendix we modify the model to remove the small signal restriction. The study of ASE is important because it bears on the question of whether ASE or SF pulses should be expected from an inverted medium and therefore on the selection of candidate nuclei for a γ-ray laser.

Trammell and Hannon (Ref. A-1) derived an expression for a pulse propagating through a gain medium of length l and attenuation coefficient μ. Assuming an incoming pulse of unit amplitude and line width Γ and corresponding lifetime $\tau = \frac{\hbar}{\Gamma}$ they concluded that the outgoing pulse, after passing through the medium, would have the form

$$I(t) = \left| A(l, t) \right|^2 = e^{-\Gamma t} I_o^2\left(\sqrt{K_o \, l \, \Gamma t \, \Delta n^*(t)}\right) e^{-\mu l} \quad , \tag{A-1}$$

where I_o is the modified Bessel function of order zero and

$$K_o = 2\pi\lambda^2 \, fg \, (1+\alpha)^{-1} \, (1+a)^{-1} \quad . \tag{A-2}$$

With $\lambda\!\!\!^{-} = \frac{\lambda}{2\pi}$, and λ the wavelength corresponding to the energy on resonance:

f is the recoilless fraction of the transition;

g is the coupling of the electromagnetic field to the nucleus;

α is the internal conversion coefficient;

a is the inhomogeneous broadening parameter;

$\Delta n^*(t) = n_1(t) - \frac{g_2}{g_1} n_2(t)$ is the inversion at time t;

$n_1(t)$, $n_2(t)$ are the populations and g_2, g_1 are the statistical factors for the two states.

Trammell and Hannon assumed that for nuclear transitions of interest to the γ-ray laser problem it was valid to replace $\Delta n^*(t)$ by the function $n_1(0)\ [2e^{-\Gamma t} - 1]$. This assumption means that the change in the level populations is determined principally by the natural lifetime and is strictly true only in the limit of small gain $K_0 \approx 1$. If the gain is large the approximation breaks down.

It is possible to deal with cases in which the gain is larger by replacing (1) with solutions of the nonlinear Haake-Reibold equations, which involve both the electric field and the polarization and which were solved numerically in Ref. A-2. However, a simpler, phenomenologically motivated numerical procedure, which operates directly on the intensity in the form given by (1), can be used to estimate the behavior of pulses as the gain is increased.

The algorithm for this purpose is based on the following considerations. The initially inverted population must be equal to the total number of photons emitted over time, i.e.,

$$N_0 = \int_0^\infty \Delta n \, dt \quad . \tag{A-3}$$

Initially

$$n_1(0) = N_0,\ n_2(0) = 0. \tag{A-4}$$

At any time t, after a time increment Δt the corresponding decrease Δn (t) in the population is the result of two processes: (1) the noninteractive emission

$$n(t)_0 \Gamma \Delta t \quad ,$$

which is due to the natural decay of individual emitters; (2) the interactive emission, which, according to (A-1) if absorption is ignored ($\mu = 0$) is given by

$$X\ (l, t - \Delta t)\ \Delta t \quad ,$$

where

$$X(l, t) = e^{-\Gamma t} I_0^2 \left[\sqrt{K_0 l\ \Gamma t\ \Delta n^* (t)} \right] \quad . \tag{A-5}$$

The algorithm begins by setting the initial conditions Eq. (A-4). Then it goes through the following steps to upgrade the quantity X (l, t) whenever the time t is incremented by an amount Δt:

1. $\Delta n = n_0(t)\,\Gamma\Delta t + X\,(l, t - \Delta t)\,\Delta t$;
2. $n_1\,(t) = n_1\,(t - \Delta t) - \Delta n\,(t)$;
3. $n_2\,(t) = n_2\,(t - \Delta t) + \Delta n\,(t)$;
4. $\Delta n^*\,(t) = n_1\,(t) - n_2\,(t)$.
5. Substitute the result of step 4 into Eq. (A-5) above.

Then the ASE, taking into account absorption, is given by

$$|\,A\,(l, t)\,|^2 = X\,(l, t)\,e^{-\mu l},$$

which follows from Eqs. (A-1) and (A-5).

For the nuclear parameters shown in Table A-1 gain is small and the pulse shown in Fig. A-1 for g = 1 appears close to the value $t \approx \frac{1}{3}\Gamma^{-1}$ as determined by Trammell and Hannon but the peak is not exactly at the value. We have found that for higher g (or larger wavelength λ) the pulses become asymmetric and shift toward shorter times, as shown in Fig. A-1. The other parameters used to calculate the pulses shown in Fig. A-1 are given in Table A-I.

Table A-1. Nominal Parameters used in the Calculations

Parameter	Symbol/units	Value
Linear attenuation coefficient	μ (cm^{-1})	0.0
Excited state lifetime	Γ (sec^{-1})	1
Recoilless fraction	f	1
Coupling Constant	g	1
Internal Conversion coefficient	α	10
Inhomogeneous broadening parameter	a	10
Wavelength on resonance	λ (cm)	10^{-8}
Number density	ρ (cm^{-3})	10^{22}
K_0	$2\pi\lambda^2 f g(1+\alpha)(1+a)^{-1}$ (cm^{-1})	1.315×10^{-19}

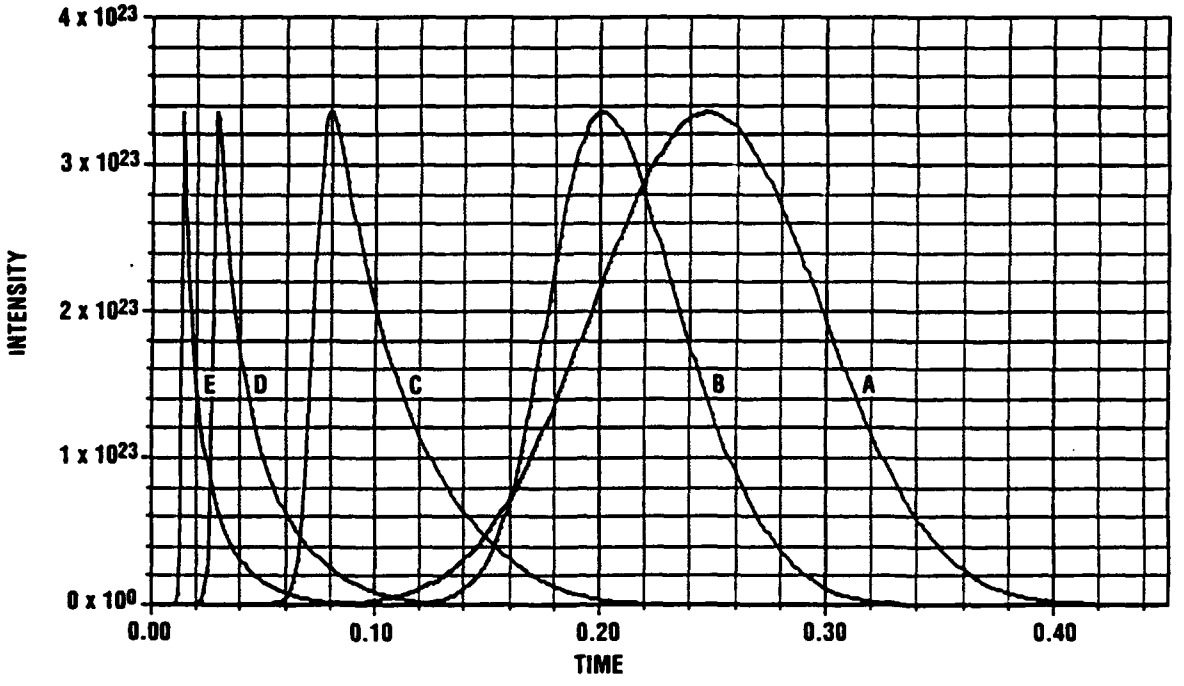

11-23-90-1

Figure A-1a. Normalized ASE pulses for different values of the coupling constant g as indicated on graph. For A, B, C, D and E, g = 1, 5, 10, 25, and 50, respectively. Only the low g value, g = 1, gives a pulse consistent with the Trammell and Hannon result, peak position at time $\frac{1}{3\Gamma}$. For the higher g values the pulses shift to the left.

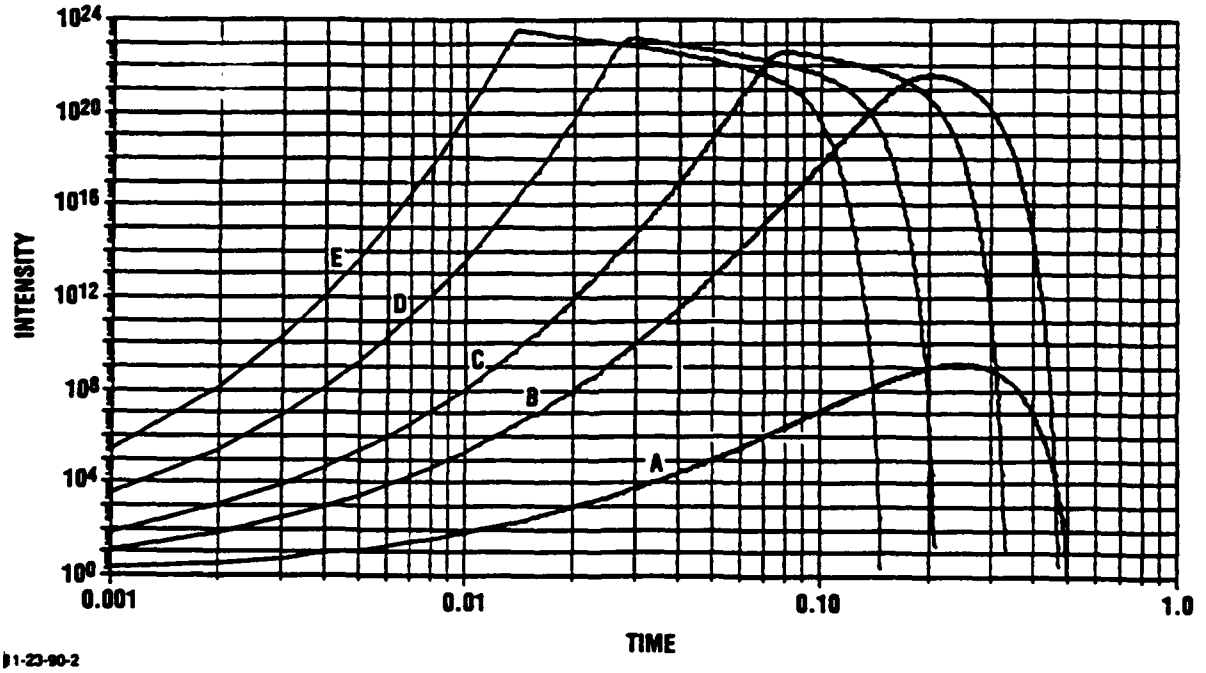

11-23-90-2

Figure A-1b. Logarithmic plot of the pulses shown in Fig. A-1a but using actual unnormalized data.

For a constant g and increasing nuclear density ρ the pulses are shown in Fig. A-2. Note that the pulses disappear between $\rho = 10^{20}$ and 10^{19}. This corresponds to the region $K_o\Delta n(0) = 13.15$ to 1.315. The pulse should disappear even for $\mu = 0$ when the condition $I_o^2(t)\left(\sqrt{K_o l\ \Gamma t\ \Delta n^*(t)}\right)e^{-\Gamma t} < 1$ is met. For this condition any effect of stimulation is overcome by the natural decay.

We also investigated the decrease in ASE as a function of μ. Figure A-3 shows pulses for $\rho = 10^{22}$ and $\rho = 10^{20}$ and different values of μ. Trammell and Hannon derived a modified Schawlow-Townes condition for the existence of ASE pulses. Their modification is to amplify the effect of μ by writing the Schawlow-Townes condition as

$$K = K_o\,\Delta n^* - M\mu > 0 \quad . \tag{A-6}$$

The factor M in front of μ results from the decrease in inversion in pulse lasers during the pulse emission. When subject to the assumption made by Trammell and Hannon that $\Delta n^*(t) = n_1(0)(2e^{\Gamma t} - 1)$, it was determined that M = 21. We do not make this assumption in our simulation studies. In our case $\Delta n^*(t)$ is calculated including the reduction by the ASE mechanism as well as natural decay. We can determine the threshold condition for lasing by determining the effect of the factor $e^{-\mu l}$ on the amplification directly by finding the value of μ for which $\left[e^{-\Gamma t}\, I_o^2\left(\sqrt{K_o l\ \Gamma t\ \Delta n^*(t)}\right)\right] e^{-\mu l}$ becomes less than one. We first calculate I(t) from equation (A-1) for $\mu = 0$ and then determine the value of μ needed to reduce I(t) at maximum to 1. We compare this to the μ calculated from the modified Schawlow-Townes condition with M = 21 [Eq. (A-6)].

Table A-2 gives the results with column 1 giving the peak intensity I(t) for $\mu = 0$, column 2 giving the threshold value of μ calculated from Eq. (A-6), column 3 giving the value of μ required in Eq. (A-1) to reduce the value in column 1 (in Table A-2) to 1, and column 4 gives the value of μ required to produce threshold condition in Eq. (A-6) with μ obtained from column 3. We use the symbol μ for the attenuation coefficient obtained from the modified Schawlow-Townes condition Eq. (A-6) and $\bar{\mu}$ for the value required in the exponent in Eq. (A-1) to reduce the pulse intensity to 1.

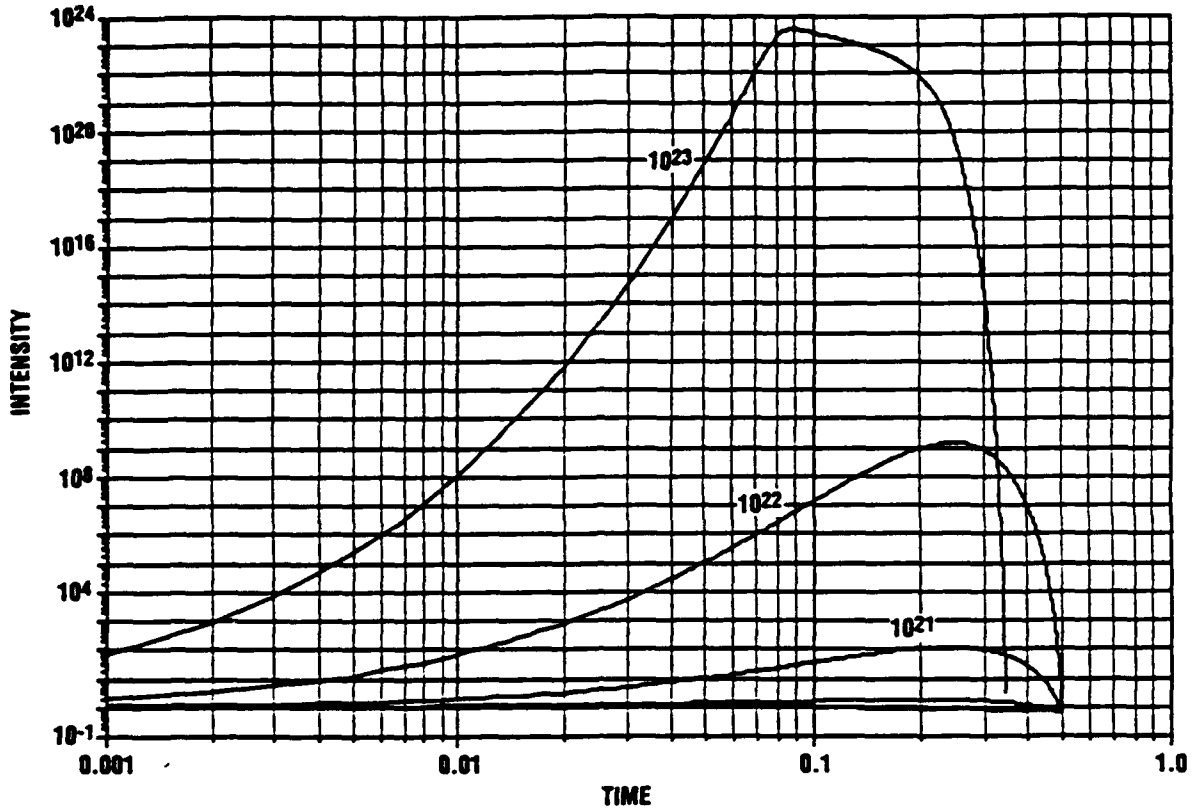

11-23-90-4

Figure A-2a. Logarithmic plot of the ASE pulses for g = 1 and different values of the initial inversion density. $\rho = 10^{20}, 10^{21}, 10^{22}, 10^{23}$.

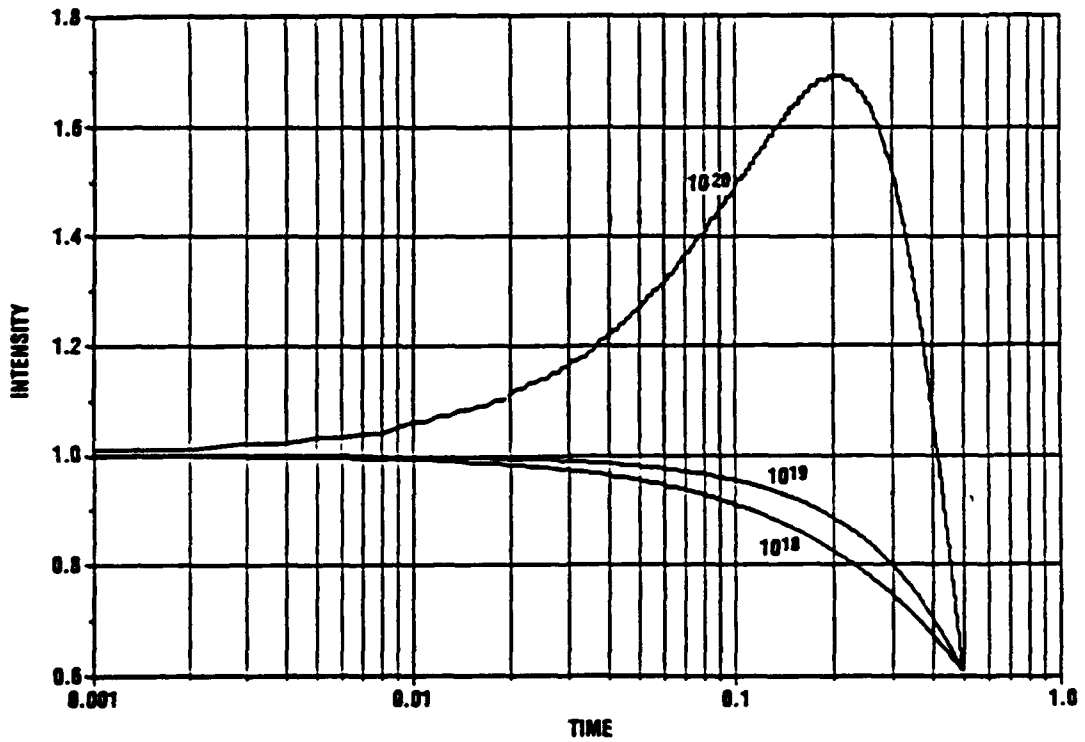

11-23-90-3

Figure A-2b. Plot of the ASE pulses for values of the initial inversion density in the threshold region between $\rho = 10^{19}$ and $\rho = 10^{20}$ cm^{-3}.

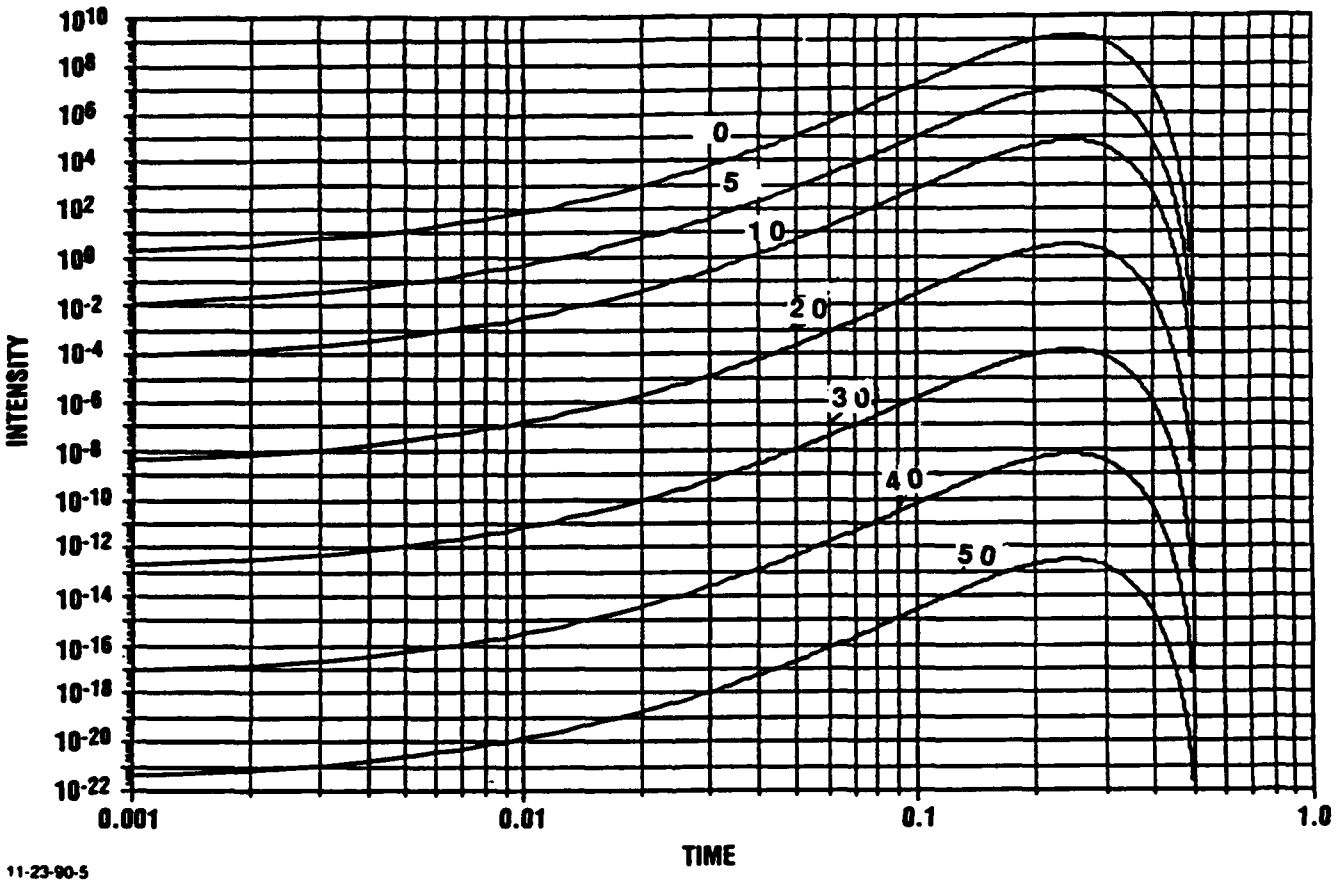

Figure A-3. Logarithmic plot of the ASE pulses for $g = 1$, $\rho = 10^{22}$ and different values of the attenuation coefficient μ as indicated on graph.

Table A-2. Threshold conditions on ASE

		(1)	(2)	(3)	(4)
			Critical attenuation coefficient μ (cm^{-1}) calculated using two approaches		Factor multiplying $\bar{\mu}$ in equation 3 for no gain
density ρ (cm^{-3})	$K_o \rho$	peak intensity* (sec^{-1}) when $\mu = 0$	From Modified S-T Condition** (μ)	$e^{\bar{\mu}}$ factor***	M
10^{23}	1.315×10^4	5×10^{23}	650	54.5	250
10^{22}	1.315×10^3	10^9	65	20.7	68
10^{21}	1.315×10^2	10^2	7.5	4.6	32
10^{20}	1.315×10	1.7	0.8	0.53	21

* Peak intensity obtained from Figure A-2.

** Critical m calculated from Eq. (A-6).

*** Critical m calculated from Eq. (A-1) assuming no amplification $|A(l, t)|^2 = 1$.

From Table A-2, we note that if we want to use the Schawlow-Townes condition the factor multiplying μ in Eq. (A-3) has to increase for systems with high gain or high density to about 250 for $\rho = 10^{23}$ cm^{-3}. Thus for ASE, M is a function of $K_o \Delta n^*$, but not a linear function. For low gain M ≈ 21 and increases roughly like $\rho^{3/2}$ for higher gain. This nonlinear behavior for threshold is expected from Eq. (A-1) where $I_o^2 \sim e^{2\sqrt{\rho}}\, e^{-\mu l}$. Figure A-3 shows ASE pulses for $\rho = 10^{22}$ and 10^{20}, g = 1 and various μ values.

The experimentally expected ASE pulse should be calculated by integrating I(t) from Eq. (A-1) over all lengths x from 0 to l to take into account the possibility that spontaneously emitted photons from all points in the active region can be amplified and contribute to the measured pulse. Thus

$$\left|A(l, t)\ \text{total}\right|^2 = \int_0^l \left|A(l-x, t)\right|^2 dx \qquad \text{(A-7)}$$

gives the expected pulse for low gain. For high gain on the other hand, a simple spontaneously emitted photon could conceivably depopulate the whole system. In this case different runs with the same initial conditions would produce different pulses and Eq. (A-1) then would represent the result of many experiments.

In Figs. A-4(a) through A-4(f) we show a surface plot of $|A(l-x,t)|^2$ as a function of x and t for $\mu = 0,5,10,20,40,80$. The volume under the surface gives $|A(l, t)\ \text{total}|^2$ and is given in Table A-3 for each value of μ along with the functions $g_1(\mu) = e^{-\mu l}$ and $g_2(\mu) = \frac{1 - e^{-\mu l}}{\mu l}$ for comparison.

The fraction $g_1(\mu)$ describes the pulse reduction after transmission over distance l and $g_2(\mu)$ describes an average reduction after transmission over different distances from 0 to l. This represents uniform source distribution in a rod and pulse emission at one end.

This volume (total intensity) calculation does not follow the approximate $\frac{1}{\mu}$ dependence obtained in the last column on the right in Table A-3 as assumed by Baldwin (Ref. A-3).

Table A-3. Parameters for Describing Pulses

μ	Volume (Total Intensity)	Normalized Volume	$e^{-\mu l}$	$\frac{1-e^{-\mu l}}{\mu l}$
0	1.3×10^{7}	1.0	1.0	1.0
5	1.0×10^{5}	1.2×10^{-2}	6.7×10^{-3}	0.2
10	3.0×10^{3}	2.3×10^{-4}	4.5×10^{-5}	0.1
20	1.2×10	9.3×10^{-7}	2.1×10^{-9}	0.05
40	1.7×10^{-1}	1.3×10^{-8}	4.2×10^{-18}	0.025
80	2.0×10^{-2}	1.5×10^{-9}	1.8×10^{-35}	0.0125

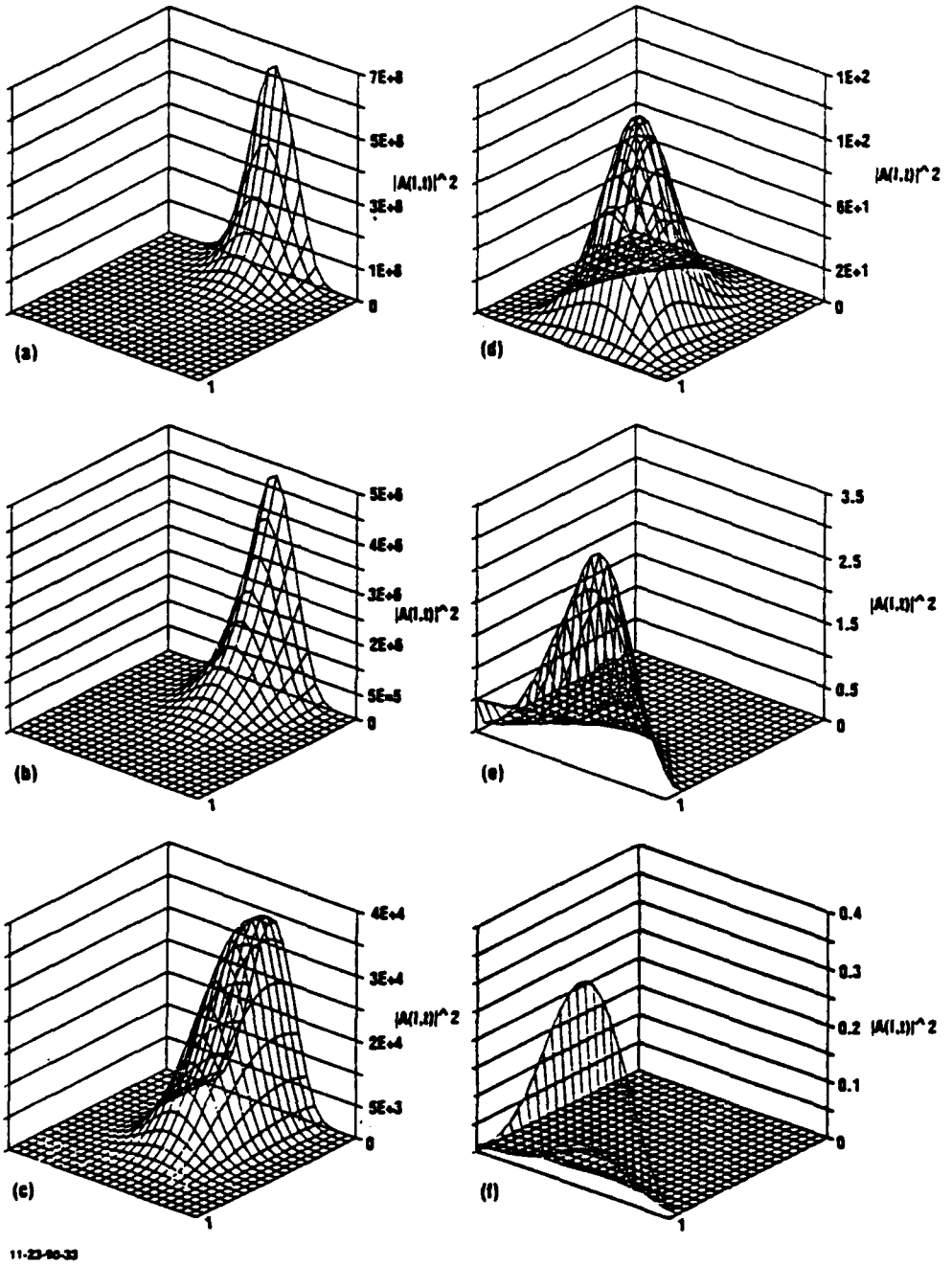

Figure A-4(a-f). A two-dimensional plot of $|A(x), t)|^2$ the pulse intensity as a function of time for different values of the attenuation coefficient μ = 0, 2, 5, 10, 20, 40, 80, shown in (a), (b), (c), (d), (e), and (f), respectively.

REFERENCES

A-1. G.T. Trammell and J.P. Hannon, "Threshold Conditions for Pulsed Gamma Ray Lasers," *Optics Comm.*, Vol. 15, No. 3, 1975, pp. 325-329.

A-2. G.C. Baldwin, "Two-Step Pumping of a Superradiant Graser," in *Proceedings of the IST/IDA Gamma Ray Laser Workshop*, B. Balko et al., eds., IDA Memorandum Report M-162, 1986, pp. 216-254.

A-3. G.C. Baldwin and R.V. Khokhlov, *Physics Today*, Vol. 28, 1975, pp. 32.